Úlfur Ágúst Atlason
25/08/2022

PI: Bert Poolman
Daily Supervisor: Sebastian Obermaier
Membrane Enzymology
University of Groningen

Experimental evolution of substrate specificity in amino acid transporters

Abstract

In yeast, amino acid transport through the cell membrane is done by Yeast Amino Acid Transporters (YAT), a family of membrane transport proteins. These proteins share a conserved structure that has diversified for a wide range of transport rate, substrates and substrate specificity. In order to explore how such diversification evolves, directed evolution can be used to explore how mutations alter those characteristics. Previous studies have used both random mutagenesis and targeted mutations to alter the substrate range of transporters. The OrthoRep system utilises orthologous replication of cytoplasmic plasmids for *in vivo* mutagenesis of target genes in *Saccharomyces cerevisiae*. The YAT Agp1 was successfully set up in this system. Two types of selective pressure were applied in parallel, towards the uptake of a new substrate, the non-canonical amino acid citrulline, and against the uptake of three toxic amino acid analogues, 4-fluorophenylalanine, 5-fluorotryptophan and β-chlorolanine. 6 new variants were successfully isolated and characterised, 2 from citrulline selection and 4 from 5-fluorotryptophan selection. Surprisingly all demonstrated the ability to take up citrulline. No improvement was observed in resistance to 5-fluorotryptophan. All variants shared the I334N mutation, bringing to question whether it predates the selection process or plays a significant role in the altered phenotype. Overall the project demonstrates a proof-of-concept of using OrthoRep for directed evolution of YATs.

Table of Contents

Introduction

A membrane separating the interior of a cell from its environment is by definition one of the fundamentals of cellular life (Bruce et al., 2008). The formation of a membrane has even been suggested as the possible first step in the origin of life, possibly with membrane spanning peptides acting in transporting and catalytic capacity (Bywater, 2009; Deamer, 2016). Such protocells would most likely require the ability to import substrates for metabolism, expel waste and do other such selective transport. Emergence of cross membrane peptides forming ion channels has been argued to be protobiologically possible due to the low sequence constraints for forming the amphipathic helices, and to a lesser extend β-barrels. Furthermore, small sequence modifications, as opposed to changes in molecular architecture, may then be sufficient to further modulate transport (Pohorille et al., 2005).

Transporters facilitate the movement of molecules through the membrane that otherwise have a low permeability. They can transport specific substrates passively down a gradient, or actively by coupling transport to the movement of ions down a gradient or ATP hydrolysis (Bruce et al., 2008). Membrane transporters are abundant proteins, constituting 2–10% of the protein types of prokaryotes, while in eukaryotes they constitute 2–7% (Brohée et al., 2010).

Nitrogen is an essential element for metabolism of organisms, being a part of essential building blocks such as amino acids and nucleotide bases. As a small, non-polar molecule, nitrogen permeates easily through membranes. However only a few bacterial species are capable of incorporating molecular nitrogen, at a high metabolic cost. Most cells hence need to import so-called fixed nitrogen through various compounds (Bruce et al., 2008). Yeast can utilise multiple compounds as sole nitrogen sources, having the enzymatic pathways to synthesise other necessary nitrogen compounds from them. Among those compounds are ammonia, urea and 17 of the 20 proteinogenic amino acids, in addition to other, non-canonical amino acids such as citrulline, ornithine, GABA, S-methylmethionine and S-adenosylmethionine. Uptake of amino acids is not only useful for nitrogen metabolism, but also reduces metabolic expense by eliminating the need of their synthesis (Bianchi et al., 2019).

In yeast, the cellular import of amino acids is primarily done by transporters of the amino acid-polyamine-choline (APC) superfamily, represented by 24 different amino acid transporters in *S. cerevisiae* (Wipf et al., 2002). Two additional transporters are of the Major Facilitator Superfamily (MFS) (Kaur and Bachhawat, 2007; Shimazu et al., 2012. Most yeast APC transporters belong to the Yeast Amino acid Transporter (YAT) family (Bianchi et al., 2019).

The YAT family transporters have a conserved structure of 12 transmembrane helixes. Many have a paralogous relationship with other members of the family, having diversified to provide different substrate specificity (Jack et al., 2000). For example, the Gap1 transporter transports all 20 proteinogenic amino acids, some additional non-proteinogenic L-amino acids and even D-amino acids, while also acting as an amino acid sensor (Donaton et al., 2003; Jauniaux and Grenson, 1990). On the other hand, the YAT Lyp1 shows high substrate specificity, only exhibiting substantial transport for lysine (Grenson, 1966). Crystal structures of bacterial APC proteins have been used to set up homology models of *S. cerevisiae* YATs. This has, along mutational studies, suggested that structural conservation of APC transporters, especially in regards to the substrate binding site, is high (Bianchi et al., 2019). Experiments have been done to elucidate how substrate specificity is created in different paralogs. Random mutagenesis of the arginine transporter Can1 has been used to create mutants capable of transporting citrulline, a substrate similar to its natural substrate arginine. Residue substitution in transmembrane helices TM3 and TM10 were capable of facilitating citrulline transfer. Interestingly it is not only mutations in the transmembrane helices that alter substrate specificity, but also in the cytosolic and extracellular loop regions (Regenberg and Kielland-Brandt, 2001). Another

experiment used the predicted binding site in Can1 to make two targeted substitutions. One substitution decreased the substrate specificity, allowing uptake of lysine in addition to arginine. The second substitution eliminated arginine transport, leaving only lysine as substrate, similar to that of YAT transporter Lyp1. This supports their model of substrate binding site in the centre of the protein structure, shaped by TM1, TM3, TM6, TM8 and TM10 (Ghaddar et al., 2014). Based on the structural similarity of YATs it is not unreasonable to assume the same applies for other YATs.

Mutational studies have been a useful tool to study the role of amino acid substitution (Bianchi et al., 2019). Using directed evolution to change substrate specificity can reveal the role of residues in substrate recognition and general transporter function (Regenberg and Kielland-Brandt, 2001). Directed evolution utilises screening for an observable selectable phenotype of a protein, inducing mutations in the gene and screening those mutants for the targeted phenotype. Random mutagenesis can be done both *in vivo* and *in vitro*. While the former is less labour-intensive it is hampered by the fact that increasing mutations *in vivo*, whether by exposure to DNA damaging conditions or replacing DNA polymerases with more error-prone versions, leads to mutation of the host genome outside the targeted gene, which reduces fitness by introducing deleterious mutations in the genome (Packer and Liu, 2015). Furthermore, false positives may be generated due to mutations in non-target genes that also enable the target phenotype (Regenberg and Kielland-Brandt, 2001).

Orthogonal replication systems, such as the OrthoRep system can sidestep this issue. It is based on a cytoplasmic plasmid system from *Kluveromyces lactis*, which has been transformed into *Saccharomyces cerevisiae.* It consists of two linear, cytoplasmic plasmids with a covalently linked tail protein (TP) on each 5'-end. The two plasmids are designated as p1 and p2. Each of these plasmids encodes a dedicated TP-DNA polymerase that is required to replicate them, while p2 has the components required for transcription. Due to the mechanical difference in using tail proteins as starting points, as well as physical separation of the plasmids from chromosomal, nuclear DNA, there is no interaction between TP-DNA polymerases and genomic DNA. Therefore, TP-DNA polymerase can be made error-prone without affecting the fidelity of genome replication (Gunge and Sakaguchi, 1981; Schaffrath et al., 1999).

Specifically, by transforming a plasmid encoding an error-prone TP-DNA polymerase for p1, and replacing the contents of plasmid p1 with a gene of interest, a system is set up where only the gene of interest is replicated with higher frequency of mutations (Ravikumar et al., 2014). The OrthoRep system has been further fine-tuned by creating additional versions of the error-prone TP-DNAP1 polymerase, allowing for modulation of mutation rate. A notable advantage of the system is its scalability, allowing for evolving genes from a bioreactor-scale down to small culture volumes in the microlitre scale (Ravikumar et al., 2018). The OrthoRep system has been used for directed evolution of a multiple-turnover THI4 thiazole synthase, found in anaerobic leech gut bacteria, for higher effectiveness under aerobic conditions with modest sulfide concentration. This adaptation allows the enzyme to function in plant-like conditions (García-García et al., 2022).

Growth of yeast in media with a specific, limited nitrogen source is an easily measurable phenotype. It can therefore be used as a selector for directed evolution of an amino acid transporter towards uptake of the specified nitrogen source. By utilising the scalability of the OrthoRep system, the target gene can be evolved under multiple selection pressures in parallel. By exploring how substrate range can be changed in different transporters, whether it can be expanded, restricted or altered we can explore how substrate specificity evolves with residue substitutions. Random mutagenesis under various separate selective pressures can be used to replicate and compare how diversification has happened in nature. This report details the setup of OrthoRep evolution system for Agp1, a broad-range, low affinity YAT (Sáenz et al., 2014; Schreve et al., 1998, p. 5). See *Figure 1* for schematics of

the setup. The scalability of the OrthoRep system allows for greater diversification compared to previous techniques, potentially allowing for testing multiple selective pressures in parallel. This report further describes the setup for applying *in vivo* selective pressure on Agp1 in yeast cultures, towards citrulline uptake, ornithine uptake and against the uptake of toxic amino acid analogues. Results of different selective pressures and the resulting mutations are compared as well.

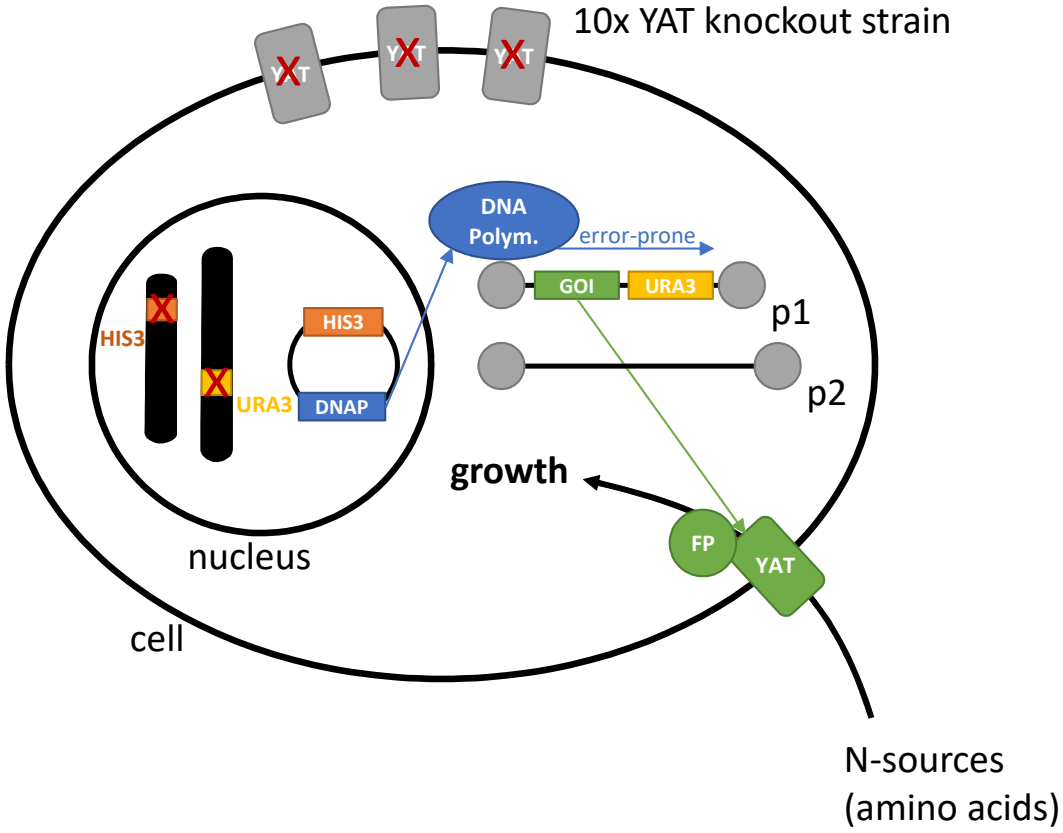

Figure 1-Schematic of OrthoRep system set up for yeast amino acid transporter as a Gene-Of-Interest. 10 amino acid transporters have previously been knocked out. Made by and used by permission of Sebastian Obermaier.

Results & Discussion

Setup of the evolution strain

Two routes were taken in parallel for setting up the platform strain, transforming error-prone TP-DNAP1 polymerase into *Saccharomyces cerevisiae strain* Δ10ΔUH. One utilised homologous recombination of TP-DNAP1 replacing a reconstituted chromosomal *URA3* gene in Δ10AA strain. The other involved introducing histidine auxotrophy by elimination of chromosomal *HIS3* gene, replacing it with *KanMX* Geneticin/G418 resistance gene. This is then followed by transformation of a TP-DNAP1 plasmid (See *Figure 2*). Two variations of TP-DNAP1 were used, plasmids pAR-Ec611 and pAR-Ec633 (Ravikumar et al., 2018).

Initial transformations were done using electro-transformation methods but did not yield success. No colonies were observed for *ura3::TP-DNAP1* transformations, and while colonies did show for *his3::KanMX* transformation, colony PCR gave no bands of the expected size (See *Figure 3*). To improve the efficiency of homologous recombination, the overhang region of both inserts was expanded. Initial size of the homologous region was 50 bp on each side of the gene. For *ura3::TP-DNAP1* the insert had

248 bp added on 5'-end and 219 bp for the 3'-end. For *his3::KanMX* a 488 bp segment is added to the 5'-end, while the amplification of the 3'-end overhang was not successful. Initial extended-overhang transformation for *ura3::TP-DNAP1* provided colonies, with one colony of pAR-Ec611 insert gave a band of the correct size (See *Figure 3*). However, attempts to cultures cells from said colony failed.

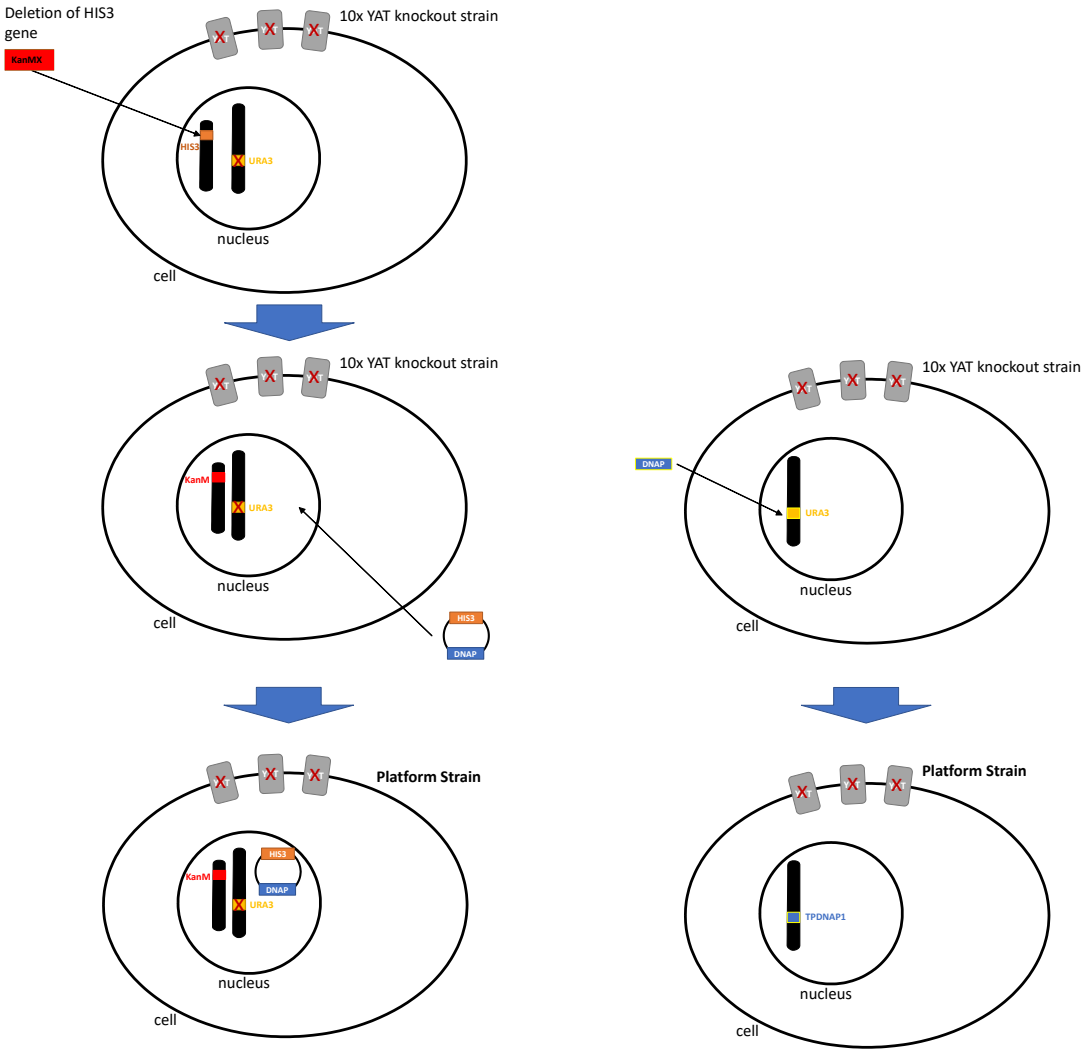

Figure 2-Two alternate setups for platform strain from Δ10AA strain*. The first path (left) eliminates* his3 *gene, which is then used as a selection marker for insertion of a plasmid with* DNAP1*. The second path (right) exchanges the* ura3 *gene with* TP-DNAP1*. Both end with a platform strain with functional* TP-DNAP1 *and an* ura3 *knockout. Adapted from scheme by Sebastian Obermaier.*

In addition to electrotransformation, protoplast transformation using the overhang-extended insert was also attempted. This gave a small (>4) number of colonies for *ura3::TP-DNAP1*, for both pAR-Ec611 and pAR-Ec633 derived inserts as well as negative control. No colonies at all appeared for *his3::KanMX* protoplast transformation. For electrotransformation, the number of *ura3::TP-DNAP1* transformant colonies was similar. However, a large number of *his3::KanMX* colonies was observed, with colony PCR showing bands at expected sizes (See *Figure 3*). Histidine auxotrophy was

demonstrated by comparing growth at varying concentrations of histidine (See *Figure 3*). Two new strains were set up from there, transformed with the pAR-Ec611 and pAR-Ec633, respectively.

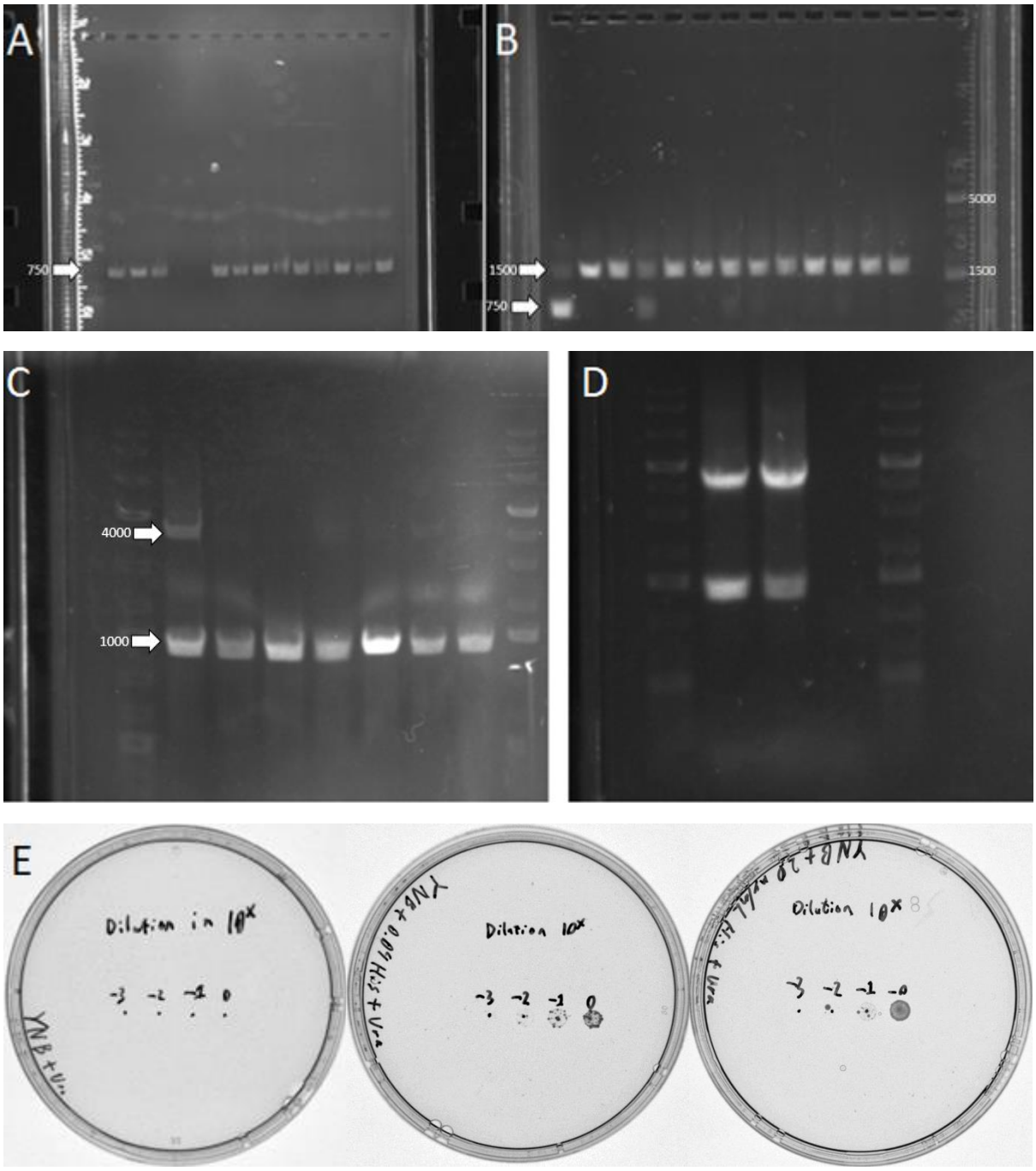

*Figure 3-Transformation of TP-DNAP1.**A**: Initial* his3::KanMX *transformation results. Only bands visible at 750 bp, instead of expected 1500. **B**: Successful* his3::KanMX *transformation. Some show the same band at 750 bp but most have a band at the expected 1500. **C**: Successful* ura3::TP-DNAP1 *transformation, the first sample shows an expected band at 4000 bp. Note that all, including negative control show band at 1500, the size of the original URA3 gene. The fact that it appears also in the negative control suggest it is contamination or background. The same thing appears in **D**, but not in the negative control. Neither colony had enough left to culture. All gels use GeneRuler 1 kb plus ladder. **E**: Growth of successful* his3::KanMX *transformation on YNB+uracil with 0, 0.04 and 2.0 mg/ml histidine.*

Four transporters were selected for transformation; *AGP1, CAN1, LYP1* and *PUT4* (*Table 1* for details on transporters). Genes were cloned into FDP-(P10B2-A75-RZ-URA3) vector and transformed into MC1061 cells, alongside empty vector. Of initial transformations, only *AGP1* was successful. The rest

of the genes was eventually successfully cloned into bacterial vectors by S. Obermaier. *Put4* and empty vector control were successfully transformed into GA-Y319 strain, but only empty vector went through successful protoplast fusion (S. Obermaier, data not published).

Table 1-Selected transporters and their sources. Adapted from Bianchi et al., 2019.

Transporter	Substrates
Agp1	Broad range
Lyp1	Lys, Met
Can1	Arg, His, Lys, Orn
Put4	Pro, Ala, Gly

For setup of the plasmid strain, *AGP1* was transformed into GA-Y319 strain, replacing p1 plasmid. Protoplast fusion was done using both pAR-Ec611 and pAR-Ec633 transformed platform strain. Plasmid strains with *AGP1* or an empty vector were fused. Only pAR-Ec611 *AGP1* fusion resulted in colony growth. The resulting strain was designated Evol-agp1.

To verify the successful transfer of plasmids onto the platform Δ10AA + Ec-611 its genome was isolated, treated with proteinase K to remove tail proteins and run on gel. Samples showed three bands in addition to genomic DNA, with sizes representing original p2 plasmid, original p1 plasmid and recombined p1 plasmid (See *Figure 4)*. To apply selective pressure against the presence of the original p1 plasmid, two colonies were grown under acidic conditions over a period of two days. DNA isolation showed two plasmids but very faint and their sizes differed from the expected size. Genome isolation in general was difficult in usage for plasmid verification as often no plasmids would be visible, despite evidence of activity of both the *AGP1* gene encoded on it as well as the *URA3* selection marker on it. Expression of Agp1 was verified by use of confocal microscopy, confirming the presence of fluorescent-marked Agp1 in the cells.

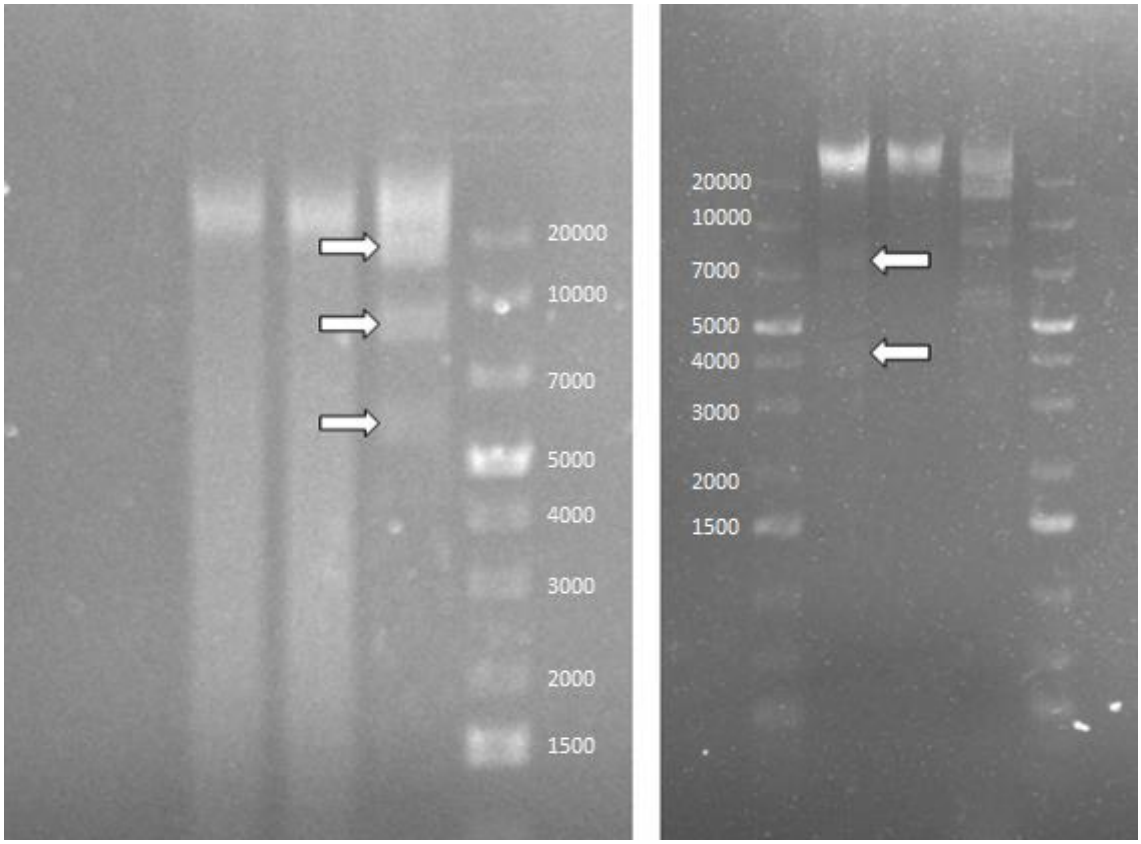

*Figure 4-**Left**: Initial DNA isolation with genomic DNA, p2 plasmid (13.5 kb), p1 WT (8.9 kb) and p1 recombinant (5.9 kb).*
***Right**: DNA isolation showing faint 2 plasmid at wrong locations (≈4.5 kb and ≈9 kb respectively).*

Initial directed evolution experiments

Pilot experiment for directed evolution was done in 96 well plate. Two colonies of Evol-agp1 that have been grown under acidic conditions for two days were inoculated into 200 µL YNB(NoN) media with different additions. For negative control Δ10AA-mKate, a Δ10AA strain with *URA3* activity reconstituted, was used. Six different canonical amino acids (0.5–3 mM), 1 non-canonical (5 mM) and two toxic amino acids analogues were tested. In addition, positive control with ammonia and negative control without nitrogen source were set up. For the toxic amino acid analogues, glutamate was used as nitrogen source. See *Table 2* for details. The 96 well plate was covered with a breathable film, and incubated while shaking. Due to condensation gathering on the film covering, OD_{600} reads were considered to be inaccurate. After one day, methodology was adapted to using no film and no shaking during incubation. The plastic cover of the plate remained. Plate was still shaken before reading, to resuspend cells, though that was later abandoned as well. A previous paper has described the growth and measurement of yeast in 96-well plates without shaking (Hung et al., 2018).

Table 2-Setup of directed evolution pilot plates.

Column	Addition	Concentration (mM)	Notes
1	NH4	76	
2	Leu	1.0	
3	Null (no nitrogen)	N/A	
4	Canavanine Glu	0.57 1.0	Nitrogen source and toxin concentration changed on third plate
5	4-Fluorophenylanaline Glu	1.0 1.0	Nitrogen source and toxin concentration changed on third plate
6	Glu	1.0	Acts as comparison for toxin wells
7	Citrulline	5.0	Not transported by Agp1
8	Met	3.0	Suboptimal growth for Δ10AA-agp1
9	Trp	3.0	Suboptimal growth for Δ10AA-agp1
10	Gly	3.0	Suboptimal growth for Δ10AA-agp1
11	Arg	0.5	
12	Gln	1.0	

The first splitting was done after three days. A clear difference between Evol-agp1 cultures and Δ10AA-mKate cultures was observed for growth in leucine, glutamate and glutamine, where Evol-agp1 cultures grew while 10ΔAA grew badly or not at all. In 5 mM citrulline the Δ10AA-mKate seemed to have advantage over the Evol-agp1, although both grew. Both strains grew equally in ammonia, methionine, tryptophan, glycine and arginine. No growth was seen without nitrogen source or in media with toxic analogues. See *Figure 5* for charted growth.

The second splitting was done after nine days. Due to complete lack of growth in toxic media its composition was readjusted. Nitrogen source was changed to leucine as growth in leucine media was comparatively better than glutamate media. Toxin concentration was also reduced tenfold. Inoculation to the new plate was done in either 100-fold or 25-fold dilution of previous culture, depending if it did or did not reach an OD_{600} exceeding 0.4 in the well. See *Figure 5* for charted growth.

The pilot study was ended after 14 days of incubation in three plates. All three plates had culture that had spilled out of the wells. As a result, the decision was made to not use 96-well plates for the setup of directed evolution experiments.

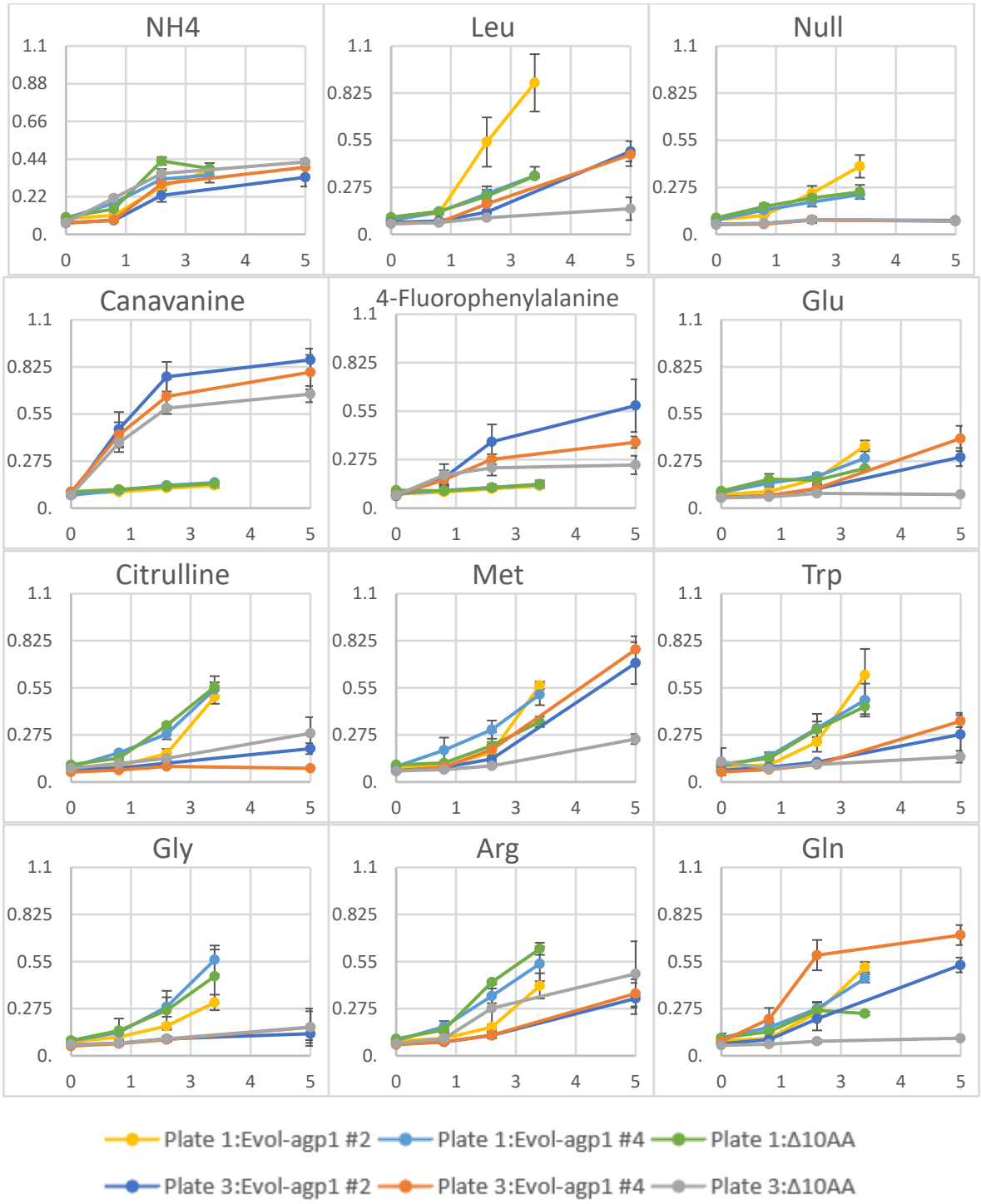

Figure 5-Initial Directed Evolution experiment. Plotted as change in OD_{600} (Y-axis) over period of days (X-axis). Comparison of growth of two inoculated colonies of Evol-agp1 and Δ10AA-mKate in different YNB(NoN) media. Note that the first plate was inoculated from YNB media, without washing, leading to nitrogen source contamination and a higher growth at low nitrogen sources, most notable in the no nitrogen Null media.

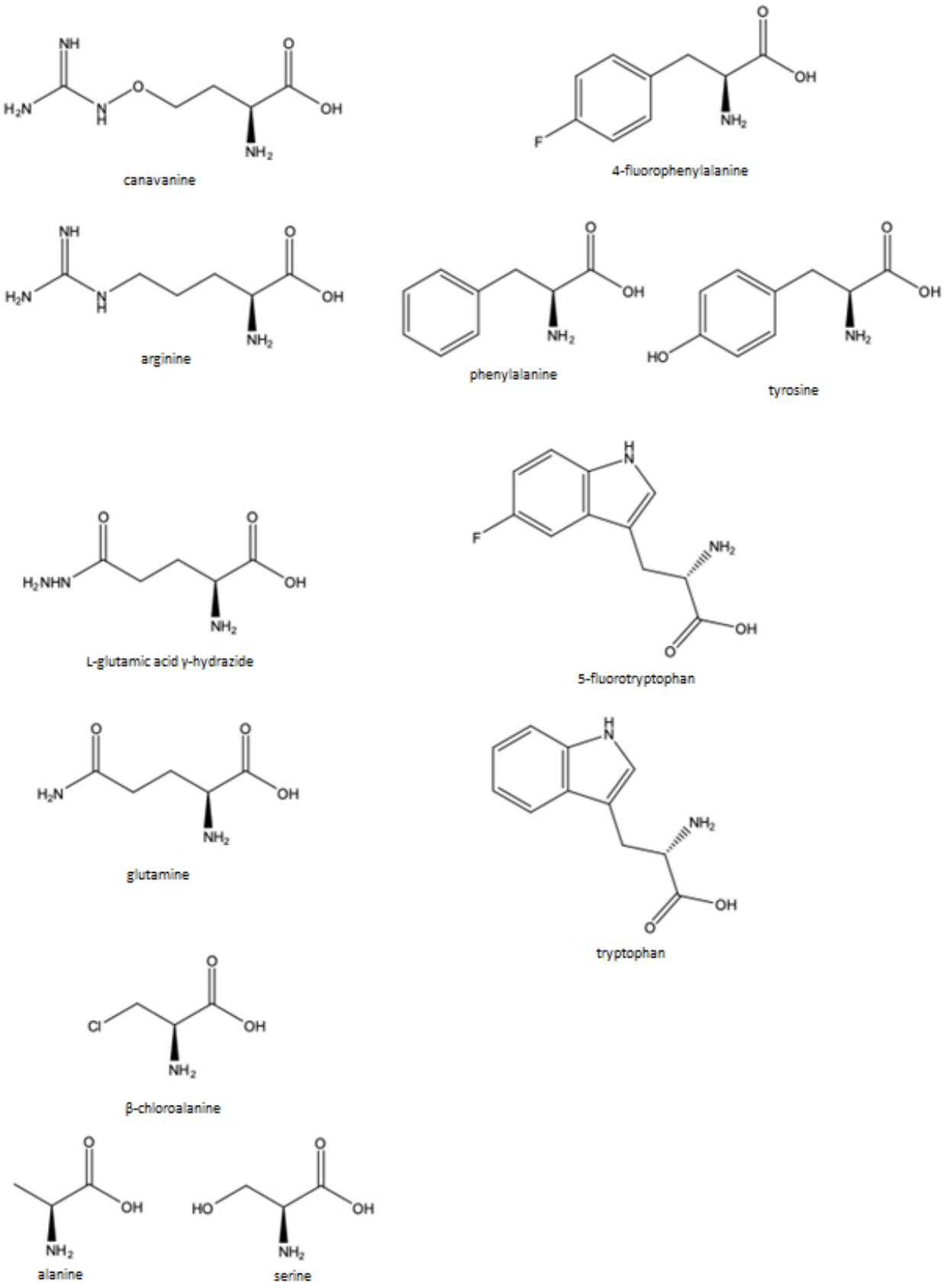

Figure 6-Comparison of toxic amino acid analogues and the amino acids they are analogous to.

Assessment of toxic amino acid analogues

Growth on toxic amino acid analogues is a traditional method for mutagenesis assay. To measure the effectiveness of mutagenesis, growth on media containing canavanine is assessed, as disabling mutations of *CAN1* gene will provide resistance to canavanine, due to its similarity to arginine (see *Figure 6*) (Lawrence, 2002). By applying the same principle, we may be able to narrow a substrate range of a transporter by selecting against the uptake of a toxic analogue, and by extension the amino acid it is analogous to.

The initial directed evolution experiment showed little difference between evol-agp1 and Δ10AA-mKate (For detailed description of strains, see Methods). Neither of the two strains could grow at high concentration of toxic analogues, while at lower concentrations the Δ10AA-mKate showed lower growth, believed to be hampered by limited nitrogen uptake. In order to effectively set up selection against toxic AA analogue uptake the minimum inhibitory concentrations had to be established. Furthermore, Agp1 must be a main contributor to uptake of said toxin for it to be possible to provide resistance to cells only by mutating *AGP1*.

First tests to establish toxin suitability were done using increasing toxin concentration in a media with multiple amino acids, designated YNB+AA media. Two toxic AA analogues were tested, 4-fluorophenylalanine and L-glutamic acid γ-hydrazide, analogues respectively to phenylalanine/tyrosine and glutamine (see *Figure 6*). Concentration range of 0.003 to 3.16 mM was tested, with 3.16-fold ($10^{0.5}$) difference between dilutions. Growth of evol-agp1 was compared to Δ10AA strains overexpressing Agp1 (Δ10AA-agp1) and not expressing it at all (Δ10AA-mKate). While Δ10AA-mKate would show worse growth due to less nitrogen uptake, the expectation was that for higher concentration of toxin, the disadvantage provided by Agp1-mediated uptake would eclipse it, especially for cells overexpressing Agp1. Improvement of growth at that concentration range would be a measurable phenotype for directed evolution. However, results showed identical growth for all cultures, growing at all concentrations of L-glutamic acid γ-hydrazide and all but the highest 4-fluorophenylalanine concentrations (see *Figure 7*). Experiment was repeated giving the same result.

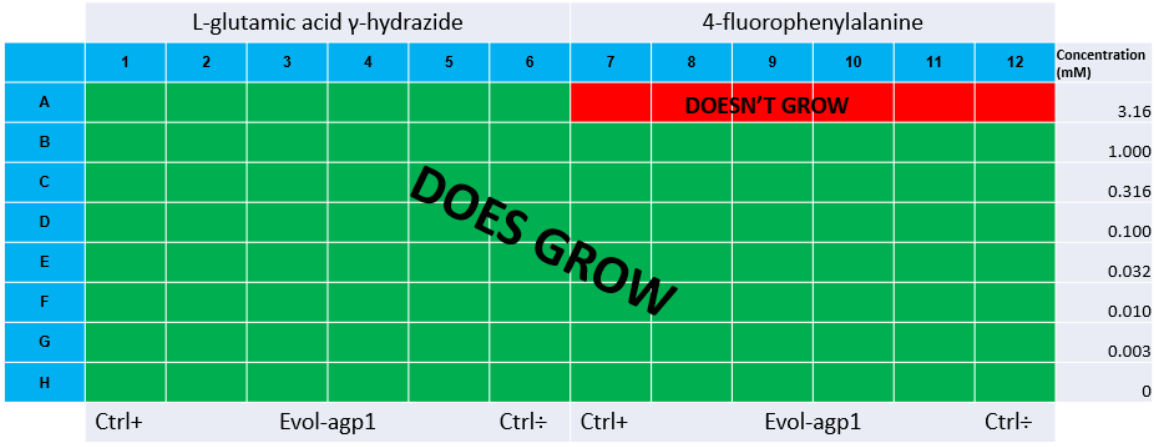

Figure 7- Schematic of a 96-well plate depicting growth after 5 days in YNB+AA media with different toxin concentrations. Ctrl+ is Δ10AA-agp1, Ctrl÷ is Δ10AA-mKate.

For the next toxin test, parameters were adjusted, exchanging YNB+AA media with YNB with 0.5 mM asparagine and 0.5 mM glutamine, designated YNB+QN media. The original rationale for using YNB+AA media was that having access to wider range of substrates in media would allow for greater phenotypic variety, allowing mutations that would eliminate uptake of multiple substrates to still remain. However, the ability of Δ10AA-mKate to grow in said media would also allow nonsense

mutations in *AGP1* to survive, and with selected toxin uptake they may even provide an advantage. Asparagine and glutamine were used as nitrogen sources, as the deletion of *AGP1* in *Δgap1 Δgnp1* yeast has been shown to inhibit the uptake of these two amino acids (Schreve et al., 1998). Furthermore, a comparison of growth in ammonia media was used to establish whether the presence of *AGP1* alters the tolerance for toxic AA analogues. The effect of three toxic AA analogues was tested; the previously mentioned 4-fluorophenylalanine (4-FPA), 5-fluorotryptophan (5-FT) and β-chloroalanine (β-CA) (See *Figure 6*).

Growth on 96 well plate was assessed visually after 1 and 5 days of growth. Evol-agp1 cultures and overexpressing Δ10AA-agp1 cells were able to grow in YNB+QN media with 0.01 mM 4-fluorophenylalanine. Miniscule growth was observed for Agp1 expressing cells in 0.1 mM 4-fluorophenylalanine as well as for Δ10AA-mKate cells. Agp1-expressing cells were able to grow in 0.1 mM 5-fluorotryptophan. Overexpressing cells showed miniscule growth in up to 10 mM 5-FTA while Δ10AA-mKate could not grow at all in these conditions. Growth in β-chloroalanine was remarkably slow, with no growth visible at all after one day of incubation. Agp1 expressing cells were able to grow at 0.01 mM, while Agp1 non-expressing cells did show miniscule growth at that toxin concentration. Agp1-overexpressing cells grew faster than evol-agp1 cells in all cases (See *Figure 8*). From this permissive concentration of toxins, allowing for cell growth, in YNB+QN media for Agp1 expressing strains is established as 0.01 mM for 4-FPA and β-CA and 0.1 mM 5-FT. Due to their miniscule growth, the permissive concentrations for Agp1 non-expressing cells could not be established for YNB+QN media.

In YNB(NoN) media with 1 mM ammonia as nitrogen source, Δ10AA-mKate cells could grow with 0.1 mM fluorophenylalanine, 0.1 mM β-chloroalanine and miniscule growth was observed in 10 mM 5-fluorotryptophan. In comparison, Δ10AA-agp1 cells in the same media were only able to grow in 0.01 mM 4-fluorophenylalanine, 0.01 mM β-chloroalanine and 0.1 mM 5-fluorotryptophan, with miniscule growth observed in 1.0 mM 5-fluorotryptophan (See *Figure 8*). The permissive concentrations of toxins for Agp1-expressing cells in YNB(NoN) with 1mM ammonia is established as the same as for YNB+QN media. The permissive concentrations for Agp1 non-expressing cells, Δ10AA-mKate, was established as higher; 0.1 mM for 4-FPA and β-CA and 1.0 mM for 5-FT. This difference demonstrates a role of Agp1 in transporting the selected toxic analogues, and possibility of variants that do not transport said toxins providing an advantage to cells.

A

4-FPA				5-FT				B-CA				Toxin Concentration (mM)
0	0	0	0	0	0	0	0	0	0	0	0	10
0	0	0	0	0	0	0	0	0	0	0	0	1
0	0	0	0	2	1	1	0	0	0	0	0	0.1
2	1	1	0	3	1	1	0	0	0	0	0	0.01
Δ10AA-agp1	Evol-agp1	Evol-agp1	Δ10AA	Δ10AA-agp1	Evol-agp1	Evol-agp1	Δ10AA	Δ10AA-agp1	Evol-agp1	Evol-agp1	Δ10AA	

B

Δ10AA-agp1				Δ10AA				Toxin Concentration (mM)
0	0	0	3	0	0	0	3	10
0	0	0	3	0	0	0	3	1
0	0	0	3	0	0	0	3	0.1
1	3	0	3	3	3	3	3	0.01
4-FPA	5-FT	β-CA	NoTox	4-FPA	5-FT	β-CA	NoTox	

C

4-FPA				5-FT				B-CA				Toxin Concentration (mM)
0	0	0	0	1	0	0	0	0	0	0	0	10
0	0	0	0	1	0	0	0	0	0	0	0	1
1	1	1	1	2	2	2	0	0	0	0	0	0.1
3	3	3	1	3	3	3	0	3	3	3	1	0.01
Δ10AA-agp1	Evol-agp1	Evol-agp1	Δ10AA	Δ10AA-agp1	Evol-agp1	Evol-agp1	Δ10AA	Δ10AA-agp1	Evol-agp1	Evol-agp1	Δ10AA	

D

Δ10AA-agp1				Δ10AA				Toxin Concentration (mM)
0	0	0	3	0	1	0	3	10
0	1	0	3	0	3	0	3	1
0	2	0	3	2	3	2	3	0.1
3	3	3	3	3	3	3	3	0.01
4-FPA	5-FT	β-CA	NoTox	4-FPA	5-FT	β-CA	NoTox	

Figure 8-Comparison of growth of Δ10AA-agp1, Evol-agp1 and Δ10AA-mKate in YNB+QN media with different concentrations of toxins after 1 (A) and 5 (C) days. Growth is scaled from 0–3 by visual inspection. On the right side is comparison of growth of Δ10AA-agp1 and Δ10AA-mKate in 1mM ammonia with different concentration of toxins after 1 (B) and 5 (D) days.

Setup of toxin selection

Toxin selection was set up in 250 mL Erlenmeyer flasks, using 100 mL YNB+QN media. Compared to the initial setup of 200 µL, this setup has vastly more volume, allowing for more cells, which allows for more possible mutants. Four cultures were set up, with 0.01 mM 4-fluorophenylalanine (4-FPA), 0.1 mM 5-fluorotryptophan (5-FT), 0.01 mM β-chloroalanine (β-CA) and a comparison culture without toxin (NoTox). Cultures were grown to stationary phase, over a period of 3-4 days, at which point they were diluted 100-fold into a new culture. The 100-fold growth is estimated to take 6–8 generations ($2^7 = 128$). This was repeated over a period of 8 weeks.

Selecting out successful mutants was done using 96-well plate with toxin concentrations of 0.01–1 mM in YNB+QN media. Growth of NoTox culture was used as comparison. Selection cultures were diluted 100-fold into 200 µL media and growth observed over a week. First selection test was done after five re-inoculations. Further selections were done after 8, 12 and 18 re-inoculations. Cultures grown in 0.01 mM 4-FPA were able to grow at 0.1 mM 4-FPA, compared to 0.01 mM for NoTox culture. Cultures grown in 0.1 mM 5-FT were able to grow at 1.0 mM 5-FT compared to 0.1 mM for NoTox culture. No increase in permissive concentration was observed for β-chloroalanine, although β-CA cultures grew faster than NoTox cultures in 0.01 mM β-CA.

To characterize the gene, it was cloned from p1 plasmid and inserted into a new expression vector by PCR. This was done from cultures that grew at improved toxin concentrations, which happened for 4-FPA and 5-FT. For the first selection plate, the gene was amplified from liquid cultures. Later cultures were spread on YNB+QN agar plates to isolate single colonies, although none of said selected colonies was successfully cloned.

The cloning procedure consisted of cloning *AGP1* into a new expression vector, pADHXC3GH. Plasmid was transformed into *E. coli* followed by isolation and transformation into Δ10AA yeast cells. In the case of the first selection plate multiple transformed bacteria colonies were kept and plasmids from them used to transform Δ10AA yeast cells. This was done to preserve diversity of single nucleotide

variance from liquid cultures, as a different variation of the plasmid may be found in different colonies. Only one plasmid was successfully cloned into Δ10AA yeast, isolated from the first selection plate growing in 1.0 mM 5-FT. Four successful transformation colonies were continued, designated XS-FT 1–4 (eXperimental Strain FluoroTryptophan), all originating after five re-inoculations. See *Figure 9* for timeline of selection process.

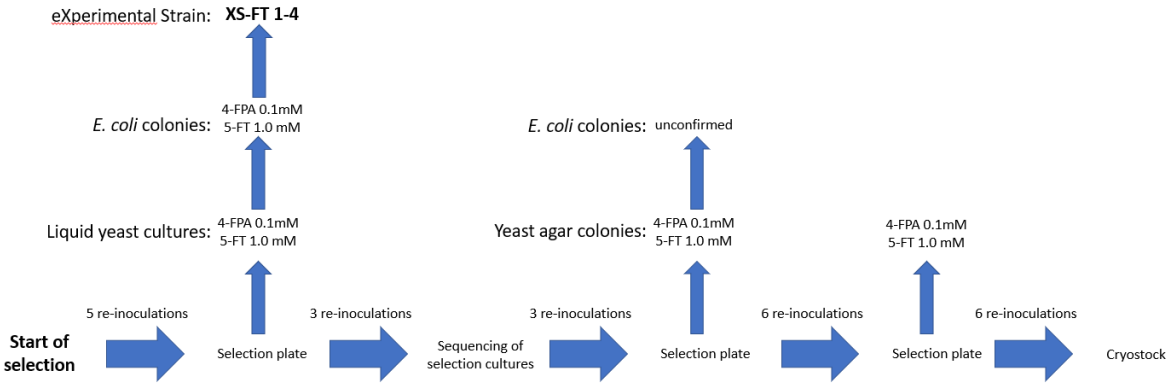

Figure 9-A flowchart describing the time point of harvesting plasmids from toxin selection. Cultures demonstrating increased toxin resistance compared to initial values were set up for cloning of plasmid, although only the first were successful. Samples of all cultures were put in cryostock at the end of the process.

Assessment of possible new substrates

As an alternative direction, the possibility of expanding the substrate range was explored. To set up a selection towards a substrate, said substrate had to fulfil three conditions; the yeast cells had to be able to utilise it as sole nitrogen source, the platform strain Δ10AA could not be able to take it up through any of the remaining amino acid transporters and Agp1 should not be able to take it up.

As a first feasibility check, cultures of Δ10AA-agp1, evol-agp1 and Δ10AA-mKate were grown in YNB+AA media, washed and spread on YNB(NoN) agar plates with 1 mM concentration of the selected substrate. This was done for two sole nitrogen sources not transported by Agp1, citrulline and ornithine. No colonies grew on citrulline plate for any strain, demonstrating that no strains were capable of taking up citrulline, with or without Agp1. Multiple colonies appeared for all strains on ornithine plates, demonstrating that transporters still present in the deletion strain are capable of transporting ornithine.

Setup of citrulline selection

10 mL cultures were set up, with YNB+AA media, a low amino acid concentration media with 3 mM citrulline (8-fold dilution of YNB+AA media diluted in YNB(NoN)) and YNB(NoN) with 3 mM ammonia. Evol-agp1 was inoculated and cultures grown to saturation, over a period of 3–4 days. At saturation, cultures were inoculated into fresh media by 20-fold dilution. This was done over a period of 8 weeks. In YNB+AA dilution with 3 mM citrulline, a low concentration of amino acids is provided, with a large reserve of citrulline. Any cells capable of utilising this reserve will be able to grow after all other nitrogen sources have been spent. Other media provide a comparison for only selection being for the continued ability to transport nitrogen, and no general selection.

Adapted mutants were selected out by plating on 1 mM citrulline plate. This was done weekly. First colonies showed after five weeks. Colonies only showed from culture grown in 3 mM citrulline, no

colonies appeared from other cultures. *AGP1* was cloned into the expression vector pADHXC3GH, same as was done for toxin selection. 11 colonies were picked, designated CitCol1-11. Three of them, CitCol5, CitCol6 and CitCol7 were transformed into Δ10AA, designated XS-Cit1, XS-Cit2 and XS-Cit3, respectively. Three later colonies, CitCol 9-11, also had plasmid cloned into an expression vector and transformed into Δ10AA, designated as XS-Cit9, XS-Cit10 and XS-Cit11. Due to time constraints no characterisation of their phenotype could be established. See *Figure 10* for details.

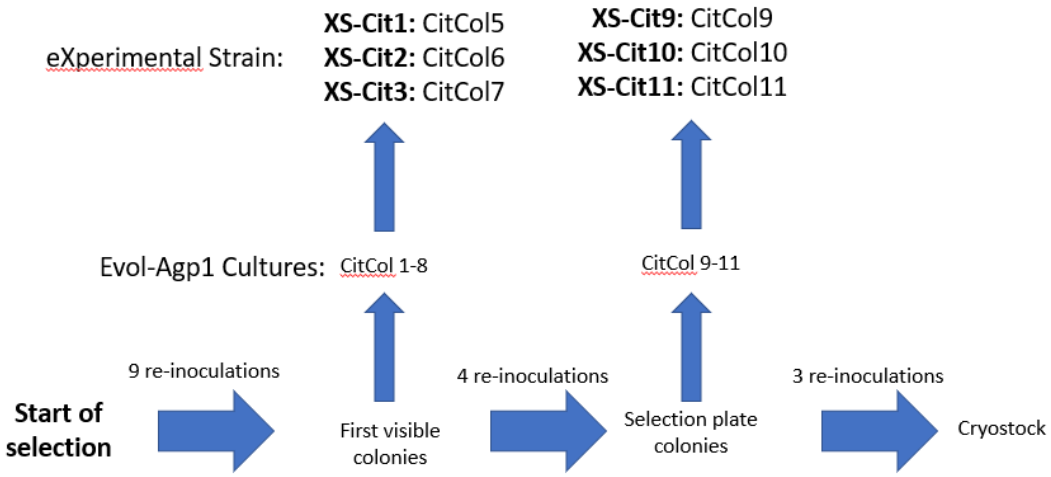

Figure 10-A flowchart describing the time point of harvesting plasmids from citrulline selection. Note that CitCol 3, 5 and 6 had the gene sequenced. A sample of culture was put in cryostock at end of the process.

Verification of Agp1 expression in XS-strains

Unmutated *AGP1* was cloned into pADHXC3GH and transformed into Δ10AA. This strain was designated XS-agp1 and used for comparison to XS-variant strains. Initial verifications of transformation of cloned *AGP1* plasmids were verified by colony PCR. The expression vector pADHXC3GH encodes a GFP tag added to the C-terminus of the protein. Therefore, expression of the protein was verified by confocal microscopy of XS-Cit 1–3 and XS-FT 1–3. For comparison XS-agp1 and Δ10AA-agp1 was observed. All XS cells showed fluorescence except XS-Cit2. Expression in Δ10AA-agp1 was much higher than in XS-agp1. It appears the pADHXC3GH vector does not show as high expression as the pDD-ADH-agp1-YPET. Fluorescence of cultures grown in YNB media and YNB+QN media was compared, with no difference found between them. See *Figure 11* for details.

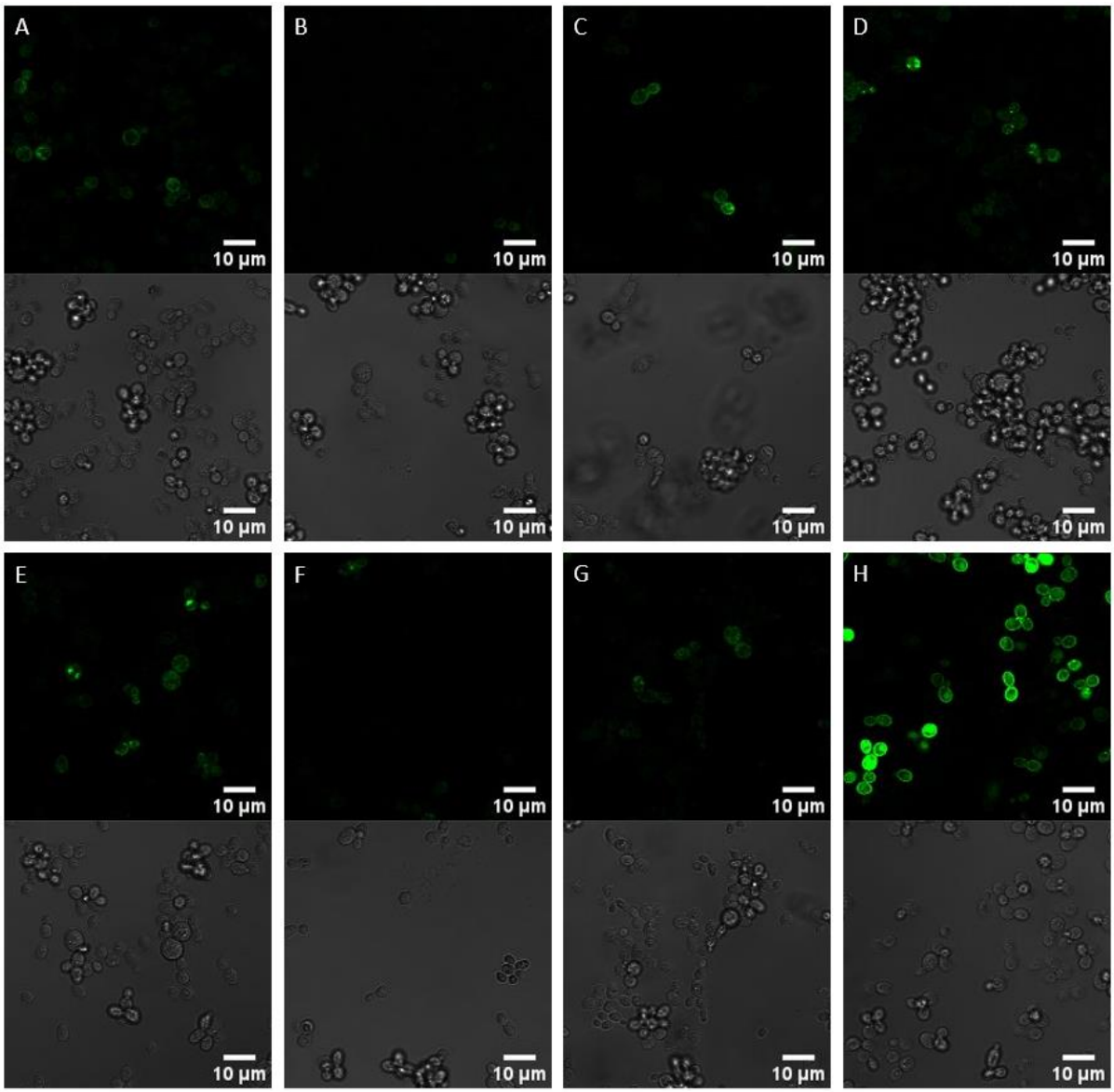

Figure 11-Confocal microscopy images, showing the fluorescence from Agp1 in XS-Cit 1–3 (A-C), XS-FT 1–3 (E-G) XS-agp1 (D) and Δ10AA-agp1 (H) All samples in YNB media.

Growth on different amino acids

Growth of all XS-strains was compared to XS-agp1, with wildtype Agp1, and WT-yeast, with all transporters functioning, on YNB+QN media with and without 1 mM 5-FT. On the plate with YNB+QN media, all strains expressing Agp1 variants grew similarly well, showing that transport of asparagine and glutamine was not impaired. On YNB+QN media with 5-FT, XS-FT mutants appeared to grow worse than XS-agp1, whereas XS-Cit mutants did not grow at all. This indicates that, contrary to what was expected, FT-mutants do not appear to have reduced uptake of 5-FT. In fact, the opposite may be true. Cit-mutants may even have increased the uptake further. 5-FT is a very different amino acid compared to citrulline. This may either mean that transport rate of the protein has increased in general, or that the transporter has become less selective, with higher affinity for various secondary substrates. See *Figure 12* for details.

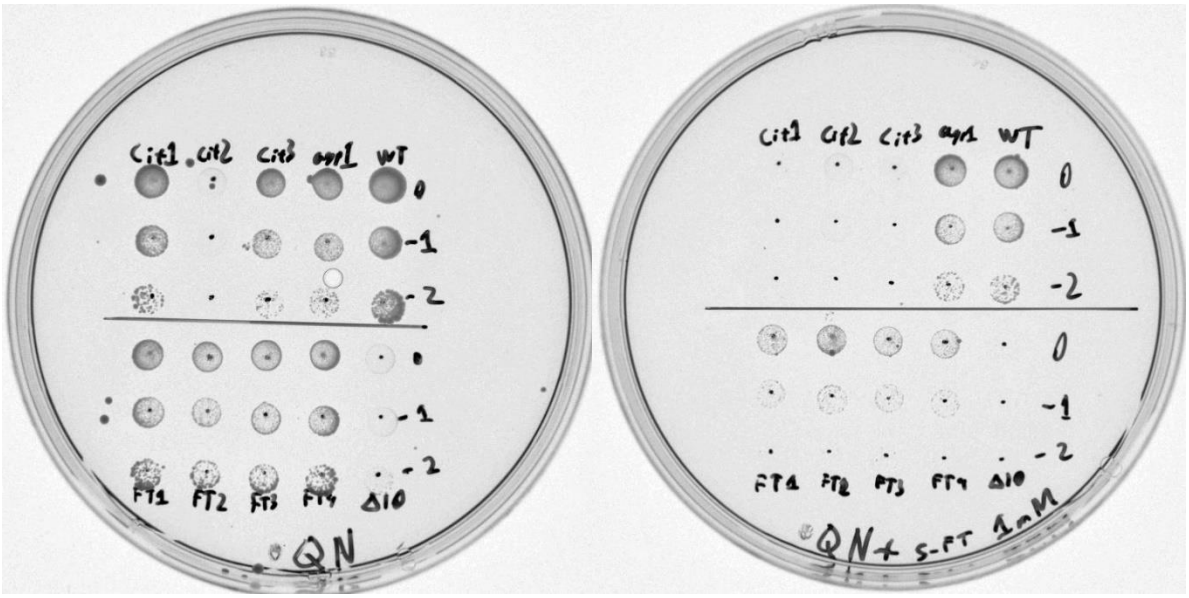

Figure 12-Comparison of growth on YNB+QN media, after 6 days, with (right) and without (left) 1 mM 5-FT. XS-FT variants show lesser growth than unmutated XS-agp1, as well as WT-yeast. XS-Cit1&3 show no growth at all on 5-FT, compared to good growth without it. XS-Cit2 doesn't grow at all on either media, similar to Δ10AA-mKate. This further indicates no presence of functional Agp1 in XS-Cit2.

XS-Cit1 and XS-Cit3 were confirmed to grow on media with 1 mM citrulline, which XS-agp1 could not. This was confirmed on 3 separate plates as well as liquid media. XS-FT variants were also confirmed to grow on citrulline. However, no *AGP1* variant could confer growth of the Δ10AA strain similar to WT-yeast. See *Figure 13* for details.

On other amino acids, XS-Cit1 and XS-Cit3 show improved growths compared to others at 1 mM GABA. GABA is similar to neither citrulline nor 5-FT, demonstrating further the apparent decrease in selectivity of Cit variants of *AGP1*. XS-FT variants show comparatively higher growth on tyrosine. This is contrary to the expectation that selection against 5-fluorotryptophan would lead to lower uptake of aromatic amino acids. All cultures grew equally on tryptophan. However, growth on tryptophan was low compared to other amino acids, as it is generally a non-ideal nitrogen source. As such it was not possible to assess if there is a notable difference of tryptophan uptake (See *Figure 14*).

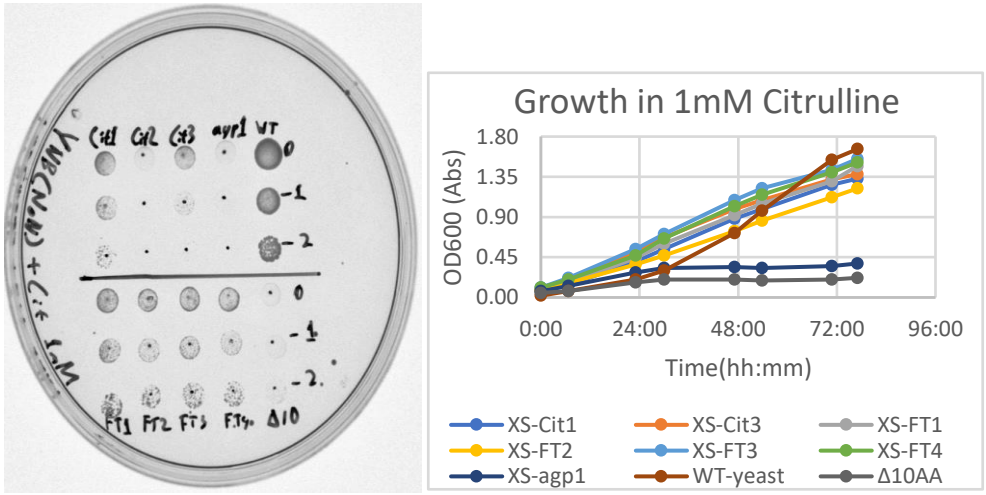

Figure 13-Growth of XS strains on 1mM citrulline. Growth on plates is pictured after 6 days. XS-Cit (excluding Cit2) and XS-FT strains grow on plate while XS-agp1 does not (left). Growth in 1mM citrulline liquid media over a period of four days shows same pattern. Note that WT-yeast was overdiluted, leading to it taking longer to catch up (right). In both, WT-yeast grows better than other strains.

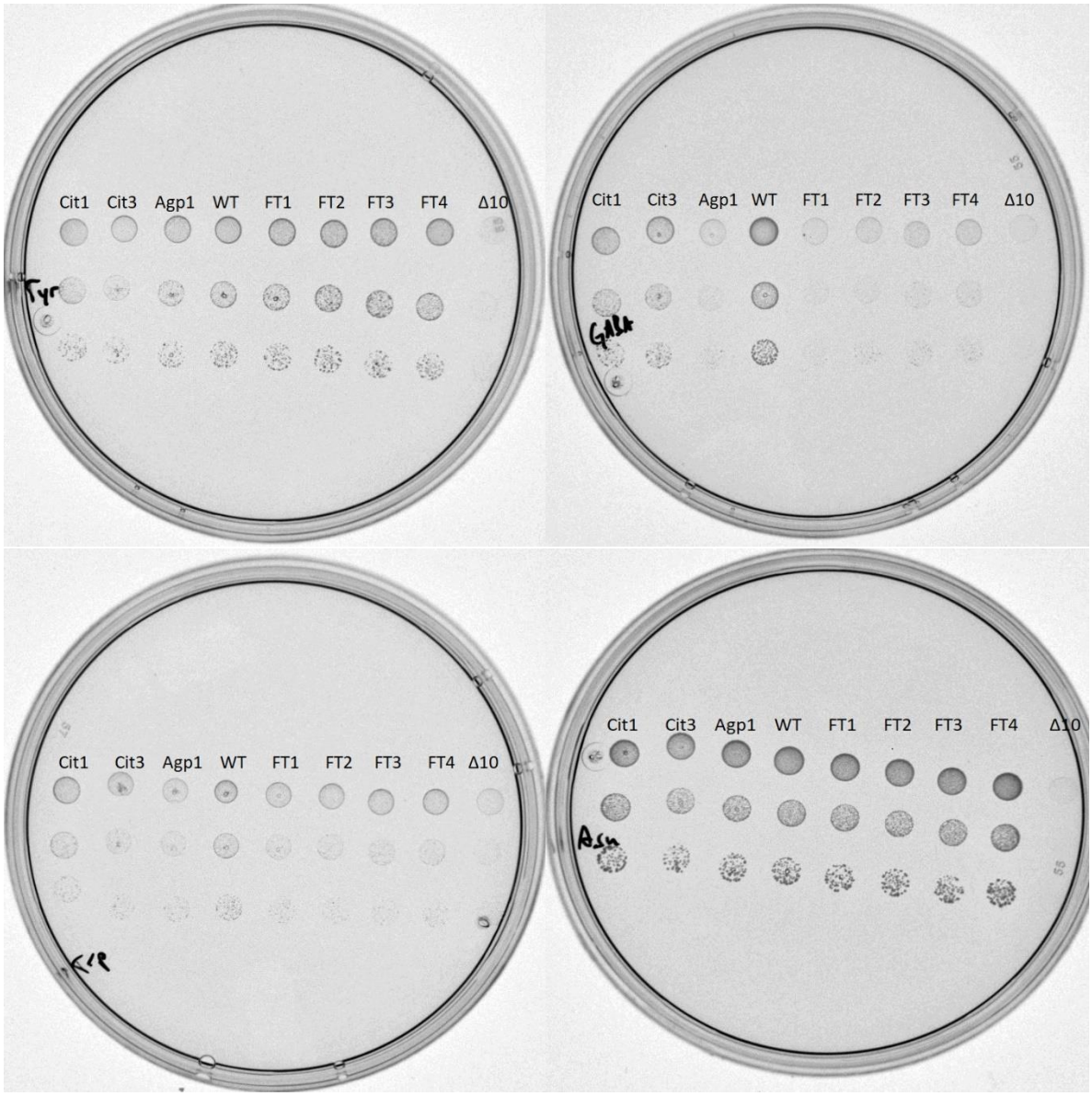

Figure 14-Comparison of growth on different nitrogen sources (YNB(NoN) + 1 mM amino acid. On GABA XS-Cit variants grow better than others except WT-yeast.On Tyr XS-FT variants appear to grow better than XS-Cit variants and XS-agp1. No difference is spotted between cultures on Trp and Asn there appears no difference, with low growth on Trp and high growth on Asn. Δ10AA-mKate does not grow on any plate.

Amino acid uptake

Uptake of citrulline was measured at concentrations of 10 µM and 50 µM, respectively over a period of 10 minutes and 3 hours. For comparison XS-agp1, Δ10AA-mKate and WT-yeast were also measured. Only WT-yeast showed measurable uptake of citrulline. Comparable measurement for uptake of glutamine showed measurable but low uptake of glutamine by all Agp1 variants (see *Figure 15*). Substrate affinity of Agp1 tends to be low, with K_m values of 0.2–0.8 mM (Bianchi et al., 2019). Measurements of citrulline uptake may be successful at higher concentrations.

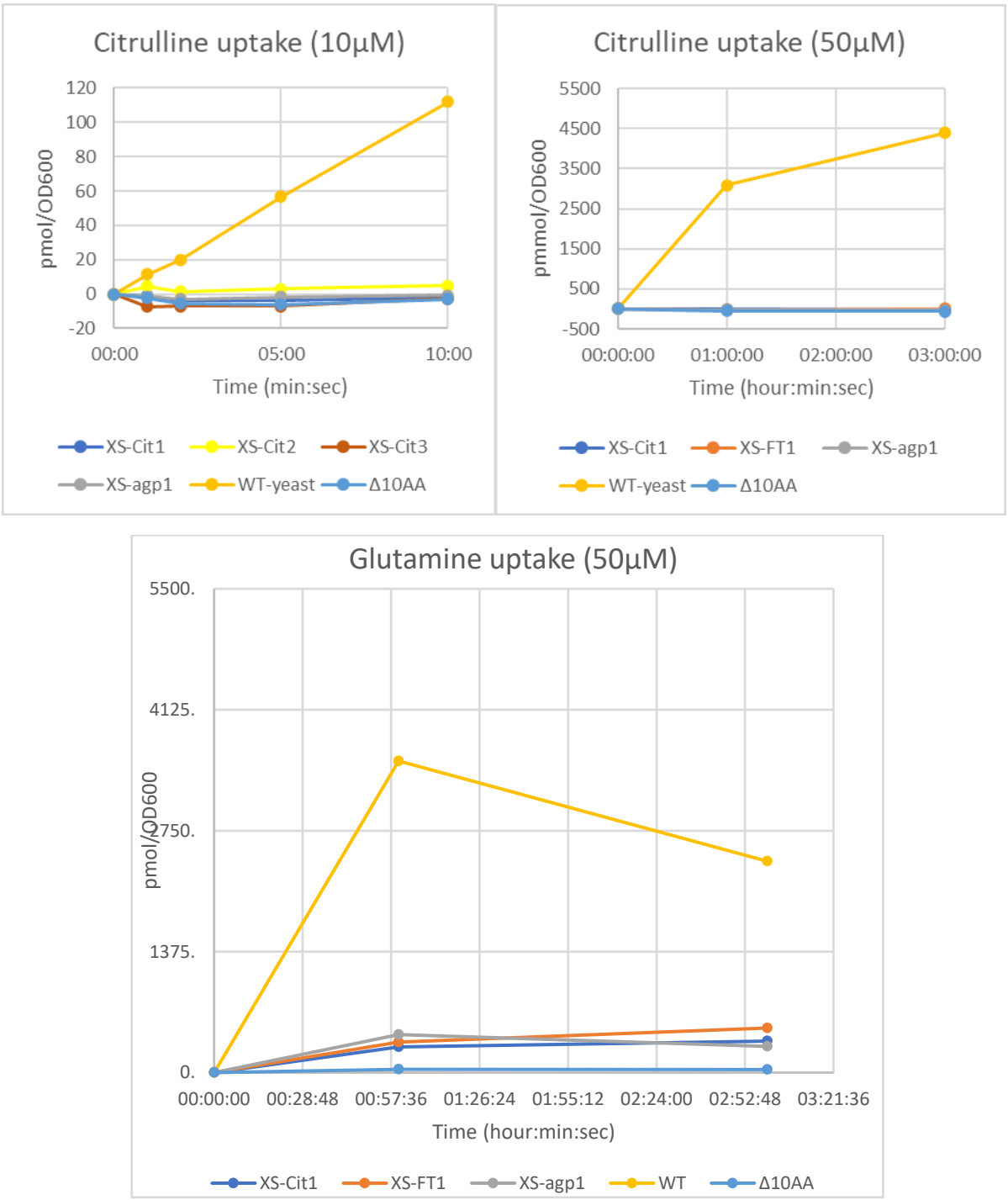

Figure 15-Uptake of citrulline and glutamine over time, adjusted for OD_{600} value. WT-yeast, presumably due to presence of high affinity transporters such as Gap1, shows a much higher uptake than XS cultures, for both substrates. No XS cultures show uptake of citrulline. XS-Cit1, XS-FT1 and XS-agp1 all show uptake of glutamine, with XS-agp1 showing faster initial uptake, dropping later.

Sequencing of cultures and expression vectors

Initial sequencing was done on samples taken from selection cultures, and the first toxin selection plate. This was after 8 and 5 rounds of re-inoculation for toxin and citrulline selection, respectively. DNA was amplified by colony PCR from liquid samples and sequenced. Single nucleotide variants (SNV) were found using INDIGO (https://www.gear-genomics.com/indigo/) online tool (Rausch et al., 2020). Reads from citrulline cultures were unreadable. Furthermore, readings from forward primers tended

to show a very high numbers of SNVs, in some cases as much as every third base showing a mutation. This is believed to be a result of the same forward primer being used for amplification and sequencing. Due to this, rate of mutations could not be assessed.

An attempt was made to improve these results by using new primers for amplification. These did not work and this delayed further sequencing. Instead sequencing primers at the start and end of the gene were used to sequence CitCol3, CitCol5 and CitCol6. Two mutations showed in all three sequences, t117c and t1001a. The former is silent, while the latter codes for a I334N substitution in the amino acid sequence. The presence of both of them in all three suggests both mutations happened early in the selection process, and may be attributed to founder effect rather than selection. Further substitutions were A484G in CitCol3, F324S in CitCol5 and N288D, F324S in CitCol6. Note that the F324S substitution in CitCol5 was a mixed read, and not present after transformation in XS-Cit1. CitCol9 and CitCol11 were isolated at the end of the citrulline selection and sequenced from transformed expression plasmids. Neither of them showed the two mutations present in Citcol 3,5 and 7. CitCol11 had 3 substitutions, S41P, A484T and I537V. CitCol9 showed a stop codon at the middle of the gene, eliminating seven of the transmembrane helices. While YAT proteins exist that have removed the two most terminal helices, removal of most of the transmembrane segments would most likely eliminate any function (Gournas et al., 2018). Neither of this variant had its function verified in XS-strain, so drawing conclusions from it may be premature.

In order to accurately sequence *AGP1* in XS-strains, sequencing was done both on plasmid used for transformation and on DNA amplified from liquid cultures. The I334N substitution and the silent t117c mutation were found in all of the XS-Cit strains. Further substitutions were I412V in XS-Cit1, located in the interior of the TM8. In XS-Cit3 there were D103G, A484G and F562L. The first two are glycine substitutions. The first one is in the first cytosolic domain, while the latter is in TM10, where its presence would probably interfere with the helix structure. TM10 contributes substantially to substrate recognition, so its disruption might lead to change in function (Ghaddar et al., 2014). The third substitution is hydrophobic-to-hydrophobic substitution in TM12, facing outwards.

All four sequenced FT variants have the same AA sequence, with substitutions F331L, I334N and A560G. The first one (F331L) is a hydrophobic-to-hydrophobic substitution situated close to I334N, also being in TM6 facing inwards into the transport pocket. The third one (A560G) is a glycine substitute at the extracellular edge of TM12. Surprisingly, the second one (I334N) is the exact same mutation found in the citrulline variants.

The FT variants had 4–6 silent mutations in addition, with the sequences of XS-FT1 being identical to XS-FT4, and XS-FT2 being identical to XS-FT3. See *Table 3* for summary of mutations and substitutions, and *Figure 16* for location of substituted residues.

Table 3-Mutations summaries for all XS variants. Substitutions mutations are in bold.

Variant	Nucleotide mutations	Amino acid substitutions
XS-Cit1	t117c **t1001a** t1191a **a1234g** t1329c c1461g t1899c	I334N I412V
XS-Cit3	t117c a308g t915c t1001a c1451g c1461g t1684c	D103G I334N A484G F562L
XS-FT1	t117c t201c t360c t563c **t991c t1001a** c1102t t1461c **c1679g**	F331L I334N A560G
XS-FT2	t117c t201c t360c **t991c t1001a** t1461c **c1679g**	F331L I334N A560G
XS-FT3	t117c t201c t360c **t991c t1001a** t1461c **c1679g**	F331L I334N A560G
XS-FT4	t117c t201c t360c t563c **t991c t1001a** c1102t t1461c **c1679g**	F331L I334N A560G

The presence of I334N in all strains (Cit and FT) as well as sequenced CitCol plasmids is surprising. There are four possibilities that could explain this. First possibility is that it is it is result of a founder effect, predating the selection process. Founder effect is an inherent risk when small populations evolve. Since growth on citrulline was not observed until after five weeks of cultivation, it would not be contributing to phenotype change. The second possibility is that I334N provides the observed phenotype. It is a hydrophobic-to-hydrophilic residue substitution in TM6, one of the helices noted to substantially contribute to substrate specificity (Ghaddar et al., 2014). The other substitutions found XS-Cit1, I412V, is a hydrophobic-to-hydrophobic substitution, found on TM8, another helix that contributes to substrate specificity. The change from isoleucine to valine, two similar amino acids would contribute less to change in the substrate environment compared to hydrophobic-to-negative charge. For XS-Cit3 the other substitutions are not obviously positioned to alter substrate specificity. The I334N substitution also occurs in FT variants, coinciding with their ability to grow on citrulline. While the citrulline selection cultures were not successfully sequenced, toxin cultures were sequenced with low but some success. While said reads provided too high number of SNVs to be valid but neither t117c and t1001a were among them. A third possibility between I334N causing the phenotype or not, would be intragenic epistasis, where additional mutation is needed to the I334N to gain the affected phenotype. An additional possibility that unfortunately cannot be ruled out, is that cross-contamination happened from citrulline cultures, which would lead to the two conserved mutations appearing in both selections.

The role of the I334N substitution could be elucidated by setting up an *AGP1* variant with only the I334N substitution and comparing its phenotype to the XS variants. Docking simulations of substrate binding would also help with assessing the role of the residue.

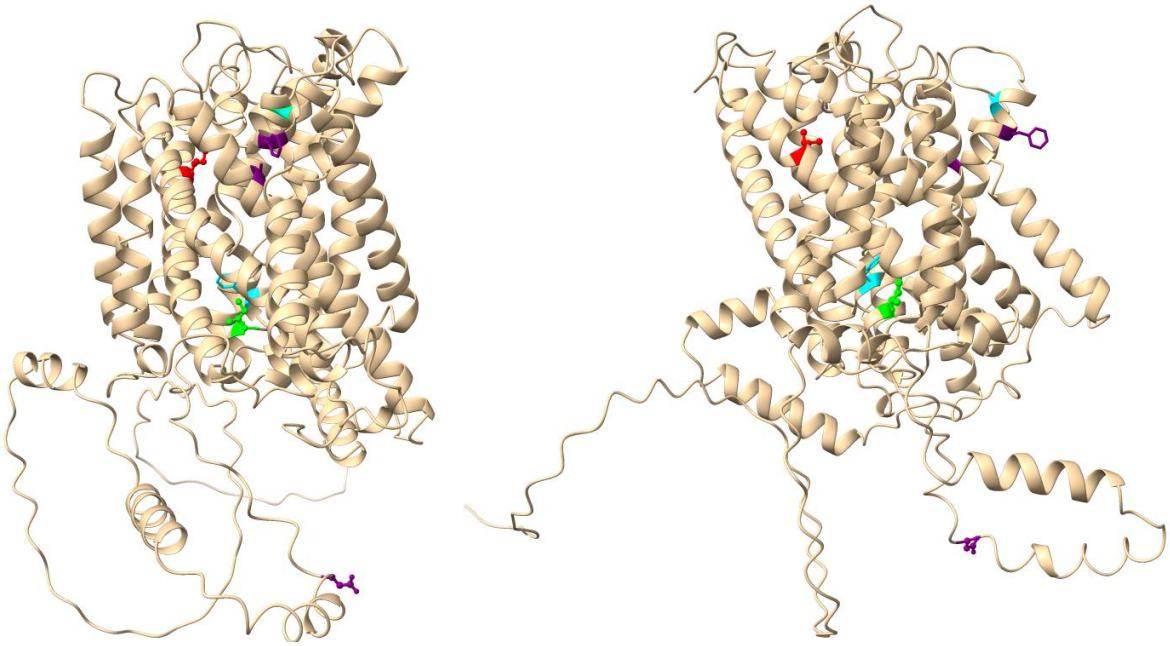

Figure 16-AlphaFold (Jumper et al., 2021; Varadi et al., 2022) model of Agp1*, with residue substitutions of XS variants highlighted. I334N marked in green, XS-Cit1 red, XS-Cit3 purple and XS-FT in cyan.*

Final notes

The attempt to mutate Agp1 to take up citrulline was successful. Interestingly, mutants selected against the uptake of 5-fluorotryptophan also proved able to take up citrulline. If I334N is not the cause of this phenotype change, it appears to be very easy to expand the substrate range of Agp1 to include citrulline. Characterising variants with only individual substitutions could further elucidate their contributions to substrate specificity.

The attempt to lower or prevent uptake of 5-fluorotryptophan, and by association tryptophan and even other aromatic amino acids was not successful. Not only were they more susceptible to 5-FT, they were also able to grow better on tyrosine. While only the variants from a single toxin selection were successfully cloned for the expression strain (4-FPA and β-CA failed), this does suggest the toxin selection setup requires improvement. The concept of mutating away from a substrate by selecting against uptake of a toxic analogue remains unproven. In both cases of citrulline selection and toxin selection, having more successful clones would provide more comparisons.

Overall, the low number of successful XS variants, with only 3 unique amino acid sequences, limited the analysis of how substrate specificity evolves. Generation of more variants could provide wider variety of mutations, perhaps giving more variety of phenotype and providing a wider viewpoint into more mutations and how they affect substrate specificity. While the OrthoRep system does simplify the creation of a library of mutants, the methodology of cloning into expression vector may require some optimisation. Difficulties of protoplast fusion remains another limiting factor.

Despite those limiting factors, the project has demonstrated a proof-of-concept for the use of the OrthoRep system and the Δ10AA knockout strain as platform for directed evolution of amino acid transporters. Further exploration is also being done on directed evolution towards more efficient uptake of substrates, as well as the setup and use of a chemostat system for more easily running different selections in parallel (S. Obermaier, data not published). This is promising for further work on using directed evolution to explore how transporter substrate specificity is controlled.

Methods

Strains

Δ10ΔUH: Platform strain with 10 amino acid transporters knocked out. Genotype: *MATα gap1-1 put4-1 uga4-1 Δcan1::HisG Δlyp1-alp1::HisG Δhip1::HisG Δdip5::HisG Δgnp1 Δagp1 Δura3::loxP Δhis3::kanMX*. Created from 22Δ10AAα.

GA-Y319: Plasmid strain containing the extranuclear p1 and p2 plasmids. Genotype: *MATα can1 his3 leu2Δ0 ura3Δ0 trp1Δ0 flo1 + p1_wt + p2_wt*. (Ravikumar et al., 2018).

Δ10AA (shorthand for 22Δ10AAα): Strain with 10 amino acid transporters knocked out. Used for experimentation of cloned transporter genes from evolution strains. Genotype: *MATα gap1-1 put4-1 uga4-1 Δcan1::HisG Δlyp1-alp1::HisG Δhip1::HisG Δdip5::HisG Δgnp1 Δagp1 ura3-1*. (Besnard et al., 2016).

Δ10AA-mKate: 22Δ10Aaα with URA3 activity restored. Used as a negative, Agp1 non-expressing control. Genotype: *MATα gap1-1 put4-1 uga4-1 Δcan1::HisG Δlyp1-alp1::HisG Δhip1::HisG Δdip5::HisG Δgnp1 Δagp1 ura3-1 + pDD-ADH-mKate2-HDEL*.

Δ10AA-agp1: 22Δ10Aaα with plasmid overexpressing Agp1, marked with an YPET tag. Used as positive, Agp1-expressing control. Genotype: *MATα gap1-1 put4-1 uga4-1 Δcan1::HisG Δlyp1-alp1::HisG Δhip1::HisG Δdip5::HisG Δgnp1 Δagp1 ura3-1 + pDD-ADH-agp1YPET.*

Evol-agp1: Evolution strain for directed evolution of Agp1 by OrthoRep system. Genotype: *MATα gap1-1 put4-1 uga4-1 Δcan1::HisG Δlyp1-alp1::HisG Δhip1::HisG Δdip5::HisG Δgnp1 Δagp1 Δura3::loxP Δhis3::kanMX + pAR-Ec611 + p1::agp1 + p2_wt*. Created from 22Δ10AAα.

WT-yeast: 23344c strain with *URA3* reinstituted. Used as a wild type comparison, expressing all regular amino acid transporters. Genotype: *Δura3 + pRS316-lyp1-Tev-YPet-his8*.

XS-agp1: Δ10AA strain with unmutated *agp1* cloned in pADHXC3GH, for comparison with eXperimental Strains. Genotype: *MATα gap1-1 put4-1 uga4-1 Δcan1::HisG Δlyp1-alp1::HisG Δhip1::HisG Δdip5::HisG Δgnp1 Δagp1 ura3-1 + pADHXC3GH-agp1-GFP*.

Media

YPD media

YPD broth powder from Formedium™ (Ref No: CCM0210) is used.

YNB media

YNB media is made with Formedium™ (Ref No: CYN0410) Yeast Nitrogen Base without amino acids powder, which is suspended and filter-sterilised. 10× and 20× concentrates were set up and diluted in sterile water. 400 g/L of glucose are autoclaved separately and added as carbon source to 20 g/L.

YNB media without a nitrogen source

YNB media without a nitrogen source, designated as YNB(NoN) is made with Formedium™ Yeast Nitrogen Base without amino acids and ammonium sulphate powder (Ref No: CYN0502), which is suspended and filter-sterilised. 10× concentrates were set up and prepared as described for YNB media.

YNB+AA media

YNB+AA media was set up by adding the amino acids to YNB(NoN). Amino acids added were leucine, isoleucine, alanine, phenylalanine, glycine, glutamate, glutamine, asparagine, aspartic acid,

methionine, proline, serine, threonine, tryptophan, valine, GABA, citrulline, ornithine at 2 mM each. Before use, media was diluted 4× for concentrations of amino acids at 0.5 mM.

YNB+QN media

YNB+QN media was set up by adding 0.5 mM each of glutamine and asparagine to YNB(NoN).

LB media

LB broth powder from Formedium™ (Ref No: LMM0102) is used. For solid media, 15 g/L agar was added before autoclaving.

TB media

TB broth powder from Formedium™ (Ref No: TBP0102) is used. After autoclaving, 10 ml of 80% glycerol is added per litre.

PCR

PCR is done with PfuX7 polymerase (Nørholm, 2010). PCR reaction is set up with Pfu 10× buffer from Agilent (Part Number:200532), 1 mM dNTPs and 1 mM $MgCl_2$. The concentration of $MgCl_2$ was later reduced to 0.25mM $MgCl_2$.

Colony PCR is done with OneTaq polymerase using 2X OneTaq MM from New England Biolabs®.

Transformation of vector into bacteria

Heat shock transformation was used to transform vectors into *E. coli* MC1061.

50 µL of competent cells were thawed on ice. They were incubated on ice for 20 minutes with ≈100 ng DNA or more. Incubation was followed by 50 second heatshock at 42 °C, 2 minutes on ice and recovery in LB media.

Ampicillin resistance was used as selector, with transformed cultures plated on LB agar plates with 100 µg/mL ampicillin sulphate.

Yeast transformation

Two different methods were used for yeast transformation, electrotransformation and lithium acetate transformation. Lithium acetate transformation was used for plasmid transformation, while electrotransformation was used for gene knockout. Protoplast transformation was also attempted once but did not yield any success (Amberg, 2022). Selective media was used depending on selection marker. For URA3 selection YNB media was used. For KanMX selection YPD media with G418 (200 µg/mL) was used.

Electrotransformation

Electrotransformation protocol was adapted from a protocol for transformation of *Hansenula polymorpha* (Faber et al., 1994). Cultures of *S. cerevisiae* were set up and reached exponential growth. Culture in exponential phase was spun down (3000 × *g*, 5 min) and resuspended in TE buffer with added 4 mg/mL DTT, in which they were incubated for 15 minutes. Cells were pelleted (3000 × *g*, 5 min, 4 °C) and washed with cold STM solution (270 mM sucrose, 10 mM Tris-HCl, 1 mM $MgCl_2$, pH 8). Following washing, the cell pellet was resuspended in the minimal amount of STM solution, to achieve a high cell density. 5 µL of DNA, concentrated by use of SpeedVac, mixed with 60 µL cell suspension was transferred to a 2 mm electroporation cuvette (PN620). Electro-pulse, using BioRad Micropulser, setting Sc2, was followed by an hour recovery period in 2xYPD, followed by washing and plating on selective plates.

Lithium acetate transformation

"High-Efficiency Transformation Protocol" as described in Gietz, 2014 was utilized. Briefly, cultures of *S. cerevisiae* were set up and grown to OD_{600} ~1.5. Culture in exponential phase was spun down (3000 × *g*, 5 min) and washed twice with sterile water, until they were resuspended in it. Plasmids are transformed using a mix of lithium acetate, PEG 3500 (Polyethylene glycol) and single stranded carrier DNA, which is then incubated for 20 minutes at 42°C.

Verification by colony PCR

Cells from colonies grown on selective media were suspended in 30 µL 2.7 mg/mL zymolyase solution, with 0.5 mm glass beads. Samples were incubated for 30–60 minutes, vortexed for 1–2 min and incubated at 95 °C before being put on ice for 5 minutes. Samples were spun down (1 min, max speed) before usage, to pellet cellular debris. Protocol was originally derived from http://sequencewww.stanford.edu/group/yeast_deletion_project/deletions3.html, accessed in 2020, but the website has become defunct since.

Protoplast fusion

Protoplast fusion was done according to protocol by García-García et al., 2022. Overnight cultures of platform and plasmid strains were grown and spun down (3000 × *g*, 5 min). Cells were resuspended in 1.4 mL 60 mM EDTA and 3 µL β-mercapoethanol, and incubated at 30 °C for 15 minutes. Cells were afterwards spun down and washed with 0.6 M KCl solution. Following this was a second incubation step in solution of 13.6 mM citric acid, 50.9 mM Na_2HPO_4, 10 mM Na_2EDTA, 0.6 M KCl and 0.27 mg/mL zymolyase, done for 1 hour at 30°C. Following this plasmid and platform strains were mixed at 1:1 ratio, centrifuged at 700 × *g*, 0 °C, 10 minutes and resuspended in 330 g/L PEG 4000, followed by incubation at 30°C for 30 minutes, with occasional inverting. Cells were pelleted and resuspended in a 0.6 M KCl, 50 mM $CaCl_2$ solution and mixed in YNB agar with 0.6 M KCl.

Genome Isolation

Genome isolation was derived from the protocol described by Amberg et al., 2005. Cells were grown to saturation overnight, and spun down at 16000 × *g*. Pellet was washed in 1 mL 0.9% NaCl, then resuspended in a solution of sorbitol 0.9 M, Na_2EDTA 0.1M, pH 7.5, and incubated with zymolyase (2.7 mg/mL) for 1 hour at 37°C. Cells were spun down at 16000 g and resuspended in 156 µl of Tris-HCl 50 mM, Na2EDTA 20 mM, pH 7.4 solution. 16 µL of 10% SDS (Sodium dodecyl sulfate), 1.7 µL 10 mg/mL proteinase K were added and solution incubated at 60 °C, 500 rpm for 30 minutes to remove tail proteins from the ends of the linear plasmids. 47 µL potassium acetate 5 M were added and the solution incubated on ice for 1 hour. Solution was then centrifuged at 16000 × *g* for 10 minutes, supernatant transferred to a new tube and mixed with two volumes 95% ethanol. Solution was then spun down at 16000 × *g* for 10 minutes, decanted, the pellet was dried at 50 °C for 30 min and resuspended in 94 µL TE (Tris-HCl 10 mM, Na_2EDTA 1 mM). After resuspension, the solution is centrifuged again at 16000 × *g* for 10 minutes, the supernatant transferred to a new tube and treated with RNase A at 37°C for 30min (1µL 5 mg/mL in supernatant). 20 µL of this solution where then run on a 0.75% agarose gel.

Growth in 96 well plates

Yeast cells were grown in 200 µL media. Plate was incubated at 30°C, with lid and without shaking. Growth was estimated by visual inspection and using well-scanning function of a BioTek340 plate reader, taking 11 OD_{600} measurement for each plate and averaging them. Usage of breathable membrane cover led to condensation issues and was discontinued. Shaking of plate risked cultures spilling out of wells and was therefore discontinued as well. Therefore, the cells were growing as a

layer at the bottom of the well, which still resulted in meaningful OD measurements. Such a setup was previously described in (Warringer and Blomberg, 2003).

Spotting assays

Grown yeast cultures were spun down and resuspended in MQ-water to a new OD_{600} value of 1.0. Two further tenfold dilutions were made from there. Of these three concentrations, 5 µL were spotted on agar plates with YNB(NoN) with different nitrogen sources and toxic amino acids added.

Confocal microscopy

Confocal microscopy was done using Zeiss LSM 710 scanning confocal microscope. Samples were grown overnight in YNB and YNB+QN media.

In vivo transport assay

Assay was performed as described previously by (Bianchi et al., 2016). Transport assay was done using ^{14}C radiolabelled citrulline, L-[ureido-^{14}C] from American Radiolabeled Chemicals, Inc. For ^{14}C-glutamine, L-[^{14}C(U)]-NEC451050UC from PerkinElmer. Glutamine was diluted 500-fold in non-radioactive glutamine. Cells were at OD_{600} of 0.5–0.7. Transport assay was in assay buffer of 100 mM potassium phosphate, 10 mM glucose at pH=6.0, incubated at 30°C. Samples were taken at fixed periods and quenched in an ice-cold assay buffer, to stop further transport. Cells were isolated by filtration onto a 0.45 µm pore size nitrocellulose filter and washed with 2 mL ice-cold assay buffer. 2 mL of scintillation solution (Emulsifier Scintillator Plus™, PerkinElmer, Waltham, MA, USA) was used to dissolve filters and measure radioactivity through liquid scintillation counting using Tri-Carb 2800TR liquid scintillation analyser from PerkinElmer.

Citations

Amberg, D., n.d. Zymolyase_Protocols [WWW Document]. URL https://resources.amsbio.com/Supporting/Zymolyase-Protocol.pdf (accessed 1.7.22).

Amberg, D.C., Burke, D., Strathern, J., 2005. Methods in yeast genetics : a Cold Spring Harbor Laboratory course manual. CSHL Press, New York, pp. 115–116.

Besnard, J., Pratelli, R., Zhao, C., Sonawala, U., Collakova, E., Pilot, G., Okumoto, S., 2016. UMAMIT14 is an amino acid exporter involved in phloem unloading in Arabidopsis roots. Journal of experimental botany J67, 6385–6397. https://doi.org/10.1093/jxb/erw412

Bianchi, F., Klooster, J.S. van 't, Ruiz, S.J., Luck, K., Pols, T., Urbatsch, I.L., Poolman, B., 2016. Asymmetry in inward- and outward-affinity constant of transport explain unidirectional lysine flux in Saccharomyces cerevisiae. Scientific Reports 6, 31443. https://doi.org/10.1038/srep31443

Bianchi, F., van't Klooster, J.S., Ruiz, S.J., Poolman, B., 2019. Regulation of Amino Acid Transport in Saccharomyces cerevisiae. Microbiology and Molecular Biology Reviews 83. https://doi.org/10.1128/MMBR.00024-19

Brohée, S., Barriot, R., Moreau, Y., André, B., 2010. YTPdb: A wiki database of yeast membrane transporters. Biochimica et Biophysica Acta (BBA) - Biomembranes 1798, 1908–1912. https://doi.org/10.1016/j.bbamem.2010.06.008

Bruce, A., Johnson, A., Lewis, J., Morgan, D., Raff, M., Roberts, K., Walter, P., 2008. Molecular Biology of The Cell. Garland Science, Taylor & Francis Group, pp. 1–10, 85–86, 597–604.

Bywater, R.P., 2009. Membrane-spanning peptides and the origin of life. Journal of Theoretical Biology 261, 407–413. https://doi.org/10.1016/j.jtbi.2009.08.001

Deamer, D., 2016. Membranes and the Origin of Life: A Century of Conjecture. Journal of Molecular Evolution 83, 159–168. https://doi.org/10.1007/s00239-016-9770-8

Donaton, M.C.V., Holsbeeks, I., Lagatie, O., Van Zeebroeck, G., Crauwels, M., Winderickx, J., Thevelein, J.M., 2003. The Gap1 general amino acid permease acts as an amino acid sensor for activation of protein kinase A targets in the yeast Saccharomyces cerevisiae. Molecular Microbiology 50, 911–929. https://doi.org/10.1046/j.1365-2958.2003.03732.x

Faber, K.N., Haima, P., Harder, W., Veenhuis, M., Ab, G., 1994. Highly-efficient electrotransformation of the yeast Hansenula polymorpha. Current Genetics 25, 305–310. https://doi.org/10.1007/BF00351482

García-García, J.D., Van Gelder, K., Joshi, J., Bathe, U., Leong, B.J., Bruner, S.D., Liu, C.C., Hanson, A.D., 2022. Using continuous directed evolution to improve enzymes for plant applications. Plant Physiology 188, 971–983. https://doi.org/10.1093/plphys/kiab500

Ghaddar, K., Krammer, E.-M., Mihajlovic, N., Brohée, S., André, B., Prévost, M., 2014. Converting the Yeast Arginine Can1 Permease to a Lysine Permease. Journal of Biological Chemistry 289, 7232–7246. https://doi.org/10.1074/jbc.M113.525915

Gietz, R.D., 2014. Yeast Transformation by the LiAc/SS Carrier DNA/PEG Method, in: Xiao, W. (Ed.), Yeast Protocols. Springer New York, New York, NY, pp. 33–44. https://doi.org/10.1007/978-1-4939-0799-1_4

Gournas, C., Athanasopoulos, A., Sophianopoulou, V., 2018. On the Evolution of Specificity in Members of the Yeast Amino Acid Transporter Family as Parts of Specific Metabolic Pathways. International Journal of Molecular Sciences 19, 1398. https://doi.org/10.3390/ijms19051398

Grenson, M., 1966. Multiplicity of the amino acid permeases in Saccharomyces cerevisiae: II. Evidence for a specific lysine-transporting system. Biochimica et Biophysica Acta (BBA) - General Subjects 127, 339–346. https://doi.org/10.1016/0304-4165(66)90388-6

Gunge, N., Sakaguchi, K., 1981. Intergeneric transfer of deoxyribonucleic acid killer plasmids, pGKl1 and pGKl2, from Kluyveromyces lactis into Saccharomyces cerevisiae by cell fusion. Journal of Bacteriology 147, 155–160. https://doi.org/10.1128/jb.147.1.155-160.1981

Hung, C.-W., Martínez-Márquez, J.Y., Javed, F.T., Duncan, M.C., 2018. A simple and inexpensive quantitative technique for determining chemical sensitivity in Saccharomyces cerevisiae. Scientific Reports 8, 11919. https://doi.org/10.1038/s41598-018-30305-z

Jack, D.L., Paulsen, I.T., Saier, M.H., 2000. The amino acid/polyamine/organocation (APC) superfamily of transporters specific for amino acids, polyamines and organocations. Microbiology (Reading) 146 (Pt 8), 1797–1814. https://doi.org/10.1099/00221287-146-8-1797

Jauniaux, J.-C., Grenson, M., 1990. GAP1, the general amino acid permease gene of Saccharomyces cerevisiae. European Journal of Biochemistry 190, 39–44. https://doi.org/10.1111/j.1432-1033.1990.tb15542.x

Jumper, J., Evans, R., Pritzel, A., Green, T., Figurnov, M., Ronneberger, O., Tunyasuvunakool, K., Bates, R., Žídek, A., Potapenko, A., Bridgland, A., Meyer, C., Kohl, S.A.A., Ballard, A.J., Cowie, A., Romera-Paredes, B., Nikolov, S., Jain, R., Adler, J., Back, T., Petersen, S., Reiman, D., Clancy, E., Zielinski, M., Steinegger, M., Pacholska, M., Berghammer, T., Bodenstein, S., Silver, D., Vinyals, O., Senior, A.W., Kavukcuoglu, K., Kohli, P., Hassabis, D., 2021. Highly accurate protein structure prediction with AlphaFold. Nature 596, 583–589. https://doi.org/10.1038/s41586-021-03819-2

Kaur, J., Bachhawat, A.K., 2007. Yct1p, a Novel, High-Affinity, Cysteine-Specific Transporter From the Yeast Saccharomyces cerevisiae. Genetics 176, 877–890. https://doi.org/10.1534/genetics.107.070342

Lawrence, C.W., 2002. Classical mutagenesis techniques, in: Guthrie, C., Fink, G.R. (Eds.), Methods in Enzymology, Guide to Yeast Genetics and Molecular and Cell Biology - Part B. Academic Press, pp. 189–199. https://doi.org/10.1016/S0076-6879(02)50963-0

Nørholm, M.H., 2010. A mutant Pfu DNA polymerase designed for advanced uracil-excision DNA engineering. BMC Biotechnology 10, 21. https://doi.org/10.1186/1472-6750-10-21

Packer, M.S., Liu, D.R., 2015. Methods for the directed evolution of proteins. Nature Reviews Genetics 16, 379–394. https://doi.org/10.1038/nrg3927

Pohorille, A., Schweighofer, K., Wilson, M.A., 2005. The Origin and Early Evolution of Membrane Channels. Astrobiology 5, 1–17. https://doi.org/10.1089/ast.2005.5.1

Rausch, T., Fritz, M.H.-Y., Untergasser, A., Benes, V., 2020. Tracy: basecalling, alignment, assembly and deconvolution of sanger chromatogram trace files. BMC Genomics 21, 230. https://doi.org/10.1186/s12864-020-6635-8

Ravikumar, A., Arrieta, A., Liu, C.C., 2014. An orthogonal DNA replication system in yeast. Nature Chemical Biology 10, 175–177. https://doi.org/10.1038/nchembio.1439

Ravikumar, A., Arzumanyan, G.A., Obadi, M.K.A., Javanpour, A.A., Liu, C.C., 2018. Scalable, Continuous Evolution of Genes at Mutation Rates above Genomic Error Thresholds. Cell 175, 1946-1957.e13. https://doi.org/10.1016/j.cell.2018.10.021

Regenberg, B., Kielland-Brandt, M.C., 2001. Amino acid residues important for substrate specificity of the amino acid permeases Can1p and Gnp1p in Saccharomyces cerevisiae. Yeast 18, 1429–1440. https://doi.org/10.1002/yea.792

Sáenz, D.A., Chianelli, M.S., Stella, C.A., 2014. L-Phenylalanine Transport in Saccharomyces cerevisiae : Participation of *GAP1, BAP2,* and *AGP1*. Journal of Amino Acids 2014, 1–9. https://doi.org/10.1155/2014/283962

Schaffrath, R., Meinhardt, F., Meacock, P.A., 1999. Genetic manipulation of Kluyveromyces lactis linear DNA plasmids: gene targeting and plasmid shuffles. FEMS Microbiology Letters 178, 201–210. https://doi.org/10.1111/j.1574-6968.1999.tb08678.x

Schreve, J.L., Sin, J.K., Garrett, J.M., 1998. The Saccharomyces cerevisiae YCC5 (YCL025c) gene encodes an amino acid permease, Agp1, which transports asparagine and glutamine. Journal of Bacteriology 180, 2556–2559. https://doi.org/10.1128/JB.180.9.2556-2559.1998

Shimazu, M., Itaya, T., Pongcharoen, P., Sekito, T., Kawano-Kawada, M., Kakinuma, Y., 2012. Vba5p, a Novel Plasma Membrane Protein Involved in Amino Acid Uptake and Drug Sensitivity in Saccharomyces cerevisiae. Bioscience, Biotechnology, and Biochemistry 76, 1993–1995. https://doi.org/10.1271/bbb.120455

Varadi, M., Anyango, S., Deshpande, M., Nair, S., Natassia, C., Yordanova, G., Yuan, D., Stroe, O., Wood, G., Laydon, A., Žídek, A., Green, T., Tunyasuvunakool, K., Petersen, S., Jumper, J., Clancy, E., Green, R., Vora, A., Lutfi, M., Figurnov, M., Cowie, A., Hobbs, N., Kohli, P., Kleywegt, G., Birney, E., Hassabis, D., Velankar, S., 2022. AlphaFold Protein Structure Database: massively expanding the structural coverage of protein-sequence space with high-accuracy models. Nucleic Acids Research 50, D439–D444. https://doi.org/10.1093/nar/gkab1061

Warringer, J., Blomberg, A., 2003. Automated screening in environmental arrays allows analysis of quantitative phenotypic profiles in Saccharomyces cerevisiae. Yeast 20, 53–67. https://doi.org/10.1002/yea.931

Wipf, D., Ludewig, U., Tegeder, M., Rentsch, D., Koch, W., Frommer, W.B., 2002. Conservation of amino acid transporters in fungi, plants and animals. Trends in Biochemical Sciences 27, 139–147. https://doi.org/10.1016/S0968-0004(01)02054-0